SECOND HARMONIC GENERATION. SEMIANNUAL TECHNICAL REPORT

James H. Boyden, et al

15 May 1971

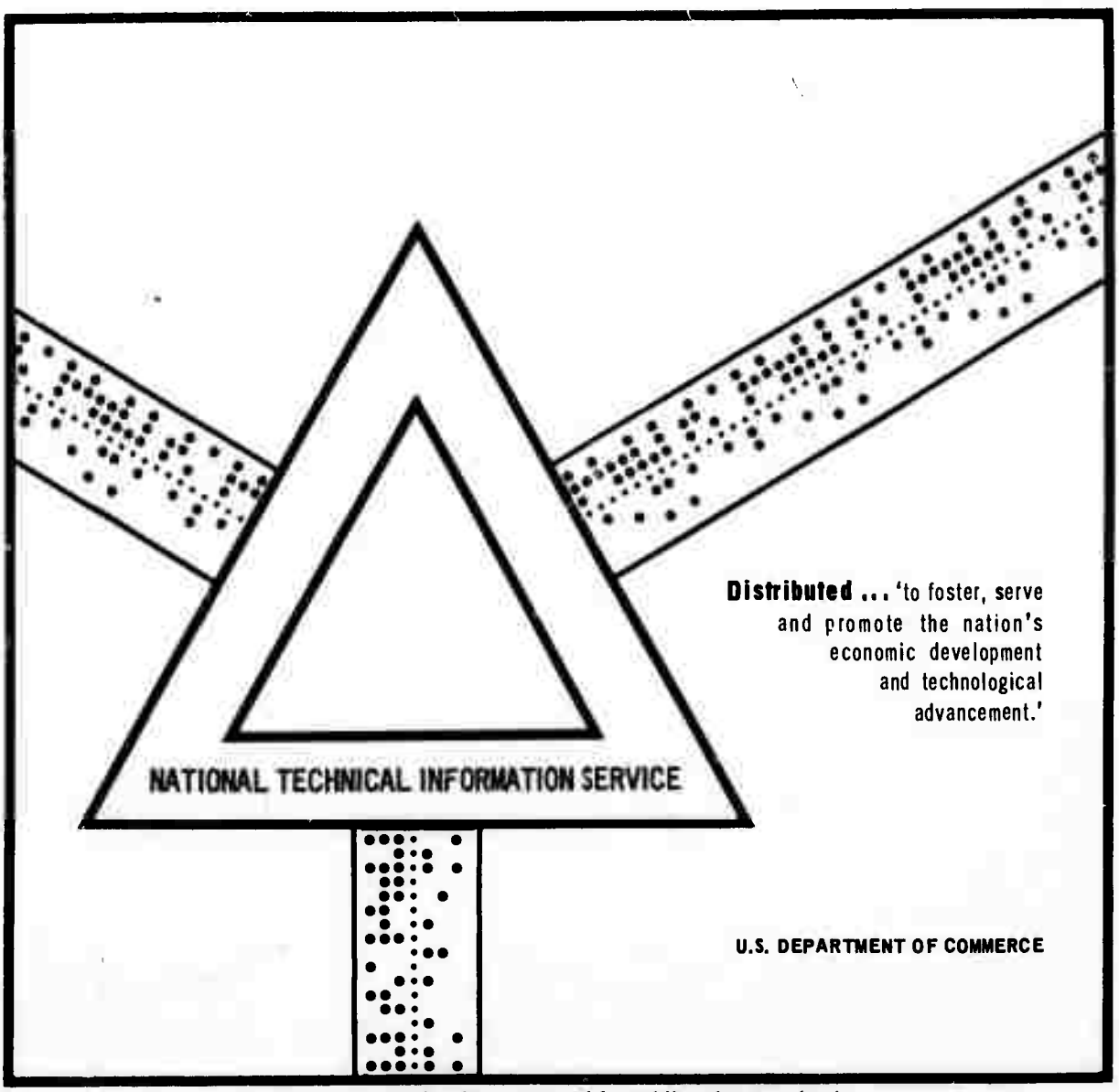

HOLOBEAM, INC.

SECOND HARMONIC GENERATION
Semiannual Technical Report
15 May 1971

ONR Contract No. N00014-71-C-0044
Program Code No. 421

Sponsored by
Advanced Research Projects Agency
ARPA Order No. 306

The Scientific Officer under this contract is the Director, Physics Programs, Physical Sciences Division, Office of Naval Research, Department of the Navy, Washington, D. C. 20360.

Duration of Contract 9/1/70 to 8/3/71
Amount of Contract $97,066.00

Program Manager

Dr. James H. Boyden

Principal Investigator

Edward G. Erickson

This research was supported by the Advanced Research Projects Agency of the Department of Defense and was monitored by ONR under Contract No. N00014-71-C-0044.

The views and conclusions contained in this document are those of the authors and should not be interpreted as necessarily representing the official policies, either expressed or implied, of the Advanced Research Projects Agency or the U.S. Government.

HOLOBEAM, INC.
560 WINTERS AVENUE
PARAMUS, NEW JERSEY 07652
Telephone 265-5335

78

Statement A per L. Jackson, ONR. A Healy
17 Sept 71

Unclassified
Security Classification

DOCUMENT CONTROL DATA - R & D

(Security classification of title, body of abstract and indexing annotation must be entered when the overall report is classified)

1. ORIGINATING ACTIVITY (Corporate author) Holobeam, Inc.	2a. REPORT SECURITY CLASSIFICATION Unclassified 2b. GROUP

3. REPORT TITLE

Second Harmonic Generation

4. DESCRIPTIVE NOTES (Type of report and inclusive dates)

Semiannual Technical Report 15May1971

5. AUTHOR(S) (First name, middle initial, last name)

Boyden, James H.; Erickson, Edward G.

6. REPORT DATE	7a. TOTAL NO. OF PAGES	7b. NO. OF REFS
15May1971	70	4

8a. CONTRACT OR GRANT NO.	9a. ORIGINATOR'S REPORT NUMBER(S)
N00014-71-C-0044 b. PROJECT NO.	Holobeam Project No. 3212
c. Program Code No. 421 d.	9b. OTHER REPORT NO(S) (Any other numbers that may be assigned this report)

10. DISTRIBUTION STATEMENT A.

11. SUPPLEMENTARY NOTES	12. SPONSORING MILITARY ACTIVITY
Details of illustrations in this document may be better studied on microfiche	Advanced Research Projects Agency ARPA Order No. 306

13. ABSTRACT

Investigations are being conducted under the subject contract with the objective of producing high average powers at a wavelength of 0.532 microns, with a short pulse and high repetition frequency format. The program objectives are to be achieved by utilizing a high average power CW Nd:YAG laser combined with electro-optic Q-switching technique and mode-locked pulse injection as a source of 1.065 micron radiation to drive a nonlinear crystal.

To date, it has been demonstrated that mode-locked pulse injection combined with Q-switching in a CW high power Nd:YAG laser can be made to function reproducibly, creating substantial increases in peak power while yielding substantial enhancement in second harmonic conversion efficiency.

The general conclusion that we have reached is that in order to produce average powers at 0.53 microns of greater than 20 watts it will be necessary to take steps to alleviate the thermal limitations of the harmonic generating crystals. This can be accomplished through an improvement in the materials themselves and the use of mechanical techniques which either distribute the thermal loading over a larger crystal volume or improve markedly the rate of heat removal. A discussion of these techniques will be presented in the final report.

DD FORM 1 NOV 65 1473 (PAGE 1)

S/N 0101-807-6801

Unclassified
Security Classification

14 KEY WORDS	LINK A		LINK B		LINK C	
	ROLE	WT	ROLE	WT	ROLE	WT
Second Harmonic Generation; Mode-Lock; Nd:YAG Laser; Q-Switch; Pockels Cell; Frequency Doubling.						

TABLE OF CONTENTS

LIST OF ILLUSTRATIONS

LIST OF ILLUSTRATIONS (Cont'd)

SECTION I

INTRODUCTION

This initial technical report summarizes the research and development efforts on Contract No. N00014-71-C-0044.. This program is directed toward the attainment of high average powers at a wavelength of 0.532 microns, with a short pulse, high repetition frequency format. The program's objectives are to be achieved by utilizing a high average power CW Nd:YAG laser combined with electro-optic Q-switching techniques and mode-locked pulse injection as a source of 1.065 micron power to drive a nonlinear crystal. Both well known and new materials are to be investigated in order to achieve high conversion efficiencies. Damage and the thermal failure of materials is an area of special concern in this program.

Our approach to the generation of high average second harmonic powers has been to develop a high average power 1.065 microns source which emits its output in a high repetition frequency high peak power format. We have accomplished this by utilizing the Holobeam developed 1000 watt CW Nd:YAG laser in conjunction with a unique electro-optical Q-switching technique combined with the injection of ultra-short pulses from a CW mode-locked Nd:YAG laser.

In order to optimally utilize the multitransverse mode output from this laser we have emphasized the utilization of 90^{o} phase-matching nonlinear materials for conversion of the 1.065 micron radiation into its second harmonic. Since the well known materials barium sodium niobate and lithium niobate have exhibited rather low damage thresholds, and potassium dideuterious phosphate does not 90^{o} phase match, we have explored in some detail the use of a new material, cesium dideuterium arsenate.

It has been demonstrated that cesium dideuterium arsenate is an efficient second harmonic converter when used in the 90^{o} phase-matching direction and operated at the phase-match temperature of approximately 100^{o}C. In excess of 25% conversion has been demonstrated for multimode polarized up conversion from 1.06μ to 0.53μ in a one cm length (single pass). It has further been shown that efficiencies in excess of 40% for a single pass can be expected in a one cm length of this material when greater mode-locking enhancement is utilized. No surface damage has been observed at non-mode-locked power densities of up to 300 mW/cm^2. 1.8 watts average green output power has been observed at a repetition rate of 100 pps and

7.2 watts average green output power has been observed at 800 pps utilizing this technique. The effect on conversion efficiency of crystal heating due to fundamental absorption has been clearly demonstrated.

A basic problem inherent in "high efficiency" frequency doubling materials has been discovered which seriously limits the use of some of these materials, such as barium sodium niobate, to the relatively unimportant role of providing efficiencies of only a few percent single pass at low power densities. This basic problem is a saturation effect which can cause the frequency doubled output to limit or actually decrease as a function of increasing power density at phase-match temperatures and at conversion efficiencies of about 12% single pass for a 5 mm length and power density of 10 mW/cm^2. It is believed that this saturation effect is in reality a two-photon absorption process wherein one photon at 1.06μ and one photon at 0.53μ is absorbed into the absorption band edge at 0.35μ. Evidence is presented later in this section supporting this conclusion. It is further speculated that this two-photon absorption process may be the basic cause of the surface damage seen with barium sodium niobate at the relatively low power densities of one or two mW/cm^2 at phase-match temperature.
(Air Force Contract No.: F 33615-69-C-1841)

Barium sodium niobate, lithium niobate, potassium dideuterium phosphate and cesium dideuterium arsenate (CD*A) have all been tested as high average power harmonic generators. No material has shown a single pass SHG efficiency higher than 14% at any power density, with the exception of CD*A, when utilizing a high divergence (10 mR) multimode pump source in spite of the theoretical difference in basic SHG efficiency of a factor of 2000 between barium sodium niobate and CD*A (per unit length and unit power density).

The laser source has been developed to the point where peak powers on the order of 5 mW are typical at pulse repetition rates in excess of 800 pps and average power outputs in excess of 80 watts. This represents pulse energies of 100 mJ/pulse. The mode-locking pulse injection system is able to provide SHG enhancement of up to a factor of 5 although the efficiency of 25% mentioned earlier was at an ennancement of only 3.

SECTION II

LASER SYSTEM

The Laser system utilized in this development program is an eight stage, single ellipse, krypton arc lamp pumped Nd:YAG laser which has produced an output in excess of 1100 watts C. W. at 1.06 microns with an input power of 48 kilowatts. The laser developed under a Holobeam internally supported program, contains 8 Nd:YAG rods, each of which are $\frac{1}{4}$" in diameter and 3 inches long. Each stage contains one rod, a single ellipse and a single pump lamp which is capable of an input power of 6kW. In the interest of a reasonable lamp lifetime, a maximum input of 5kW is normally utilized which provides an output for all eight stages of between 760 and 800 watts. Output curves are shown in Figure 2-1.

The typical beam divergence at 800 watts is 15mR, although a beam divergence of 5mR was obtained at an output power of 500 watts, utilizing a slightly modified version. The overall dimension of the laser head chain is 4 inches x 4 inches x 62 inches.

2.1 Q-Switched Operation

The problems associated with "Q" switching a continuously pumped Nd:YAG laser are primarily caused by an induced thermal optic birefringence which becomes more severe as the pumping power and presumably the C. W. output power is increased in any given system. This birefringence in most cases eliminates or at least severely limits the utilization of a Pockels cell as the "Q" switching mechanism due to the basic requirement that the laser must be internally polarized. We report here on a technique which utilizes this birefringence as an output coupling mechanism for a C. W. pumped laser which has both a high gain and a high coupling coefficient between states of polarization, that is, a high degree of birefringence.

We have measured the single pass gain of the system at a pump level of 5kW/1amp by inserting a one-half watt C. W. beam from another YAG laser after removing the mirrors from the main system. The measured output was 8 watts, implying a single pass small signal gain of 16 and a double pass gain of 256 which is

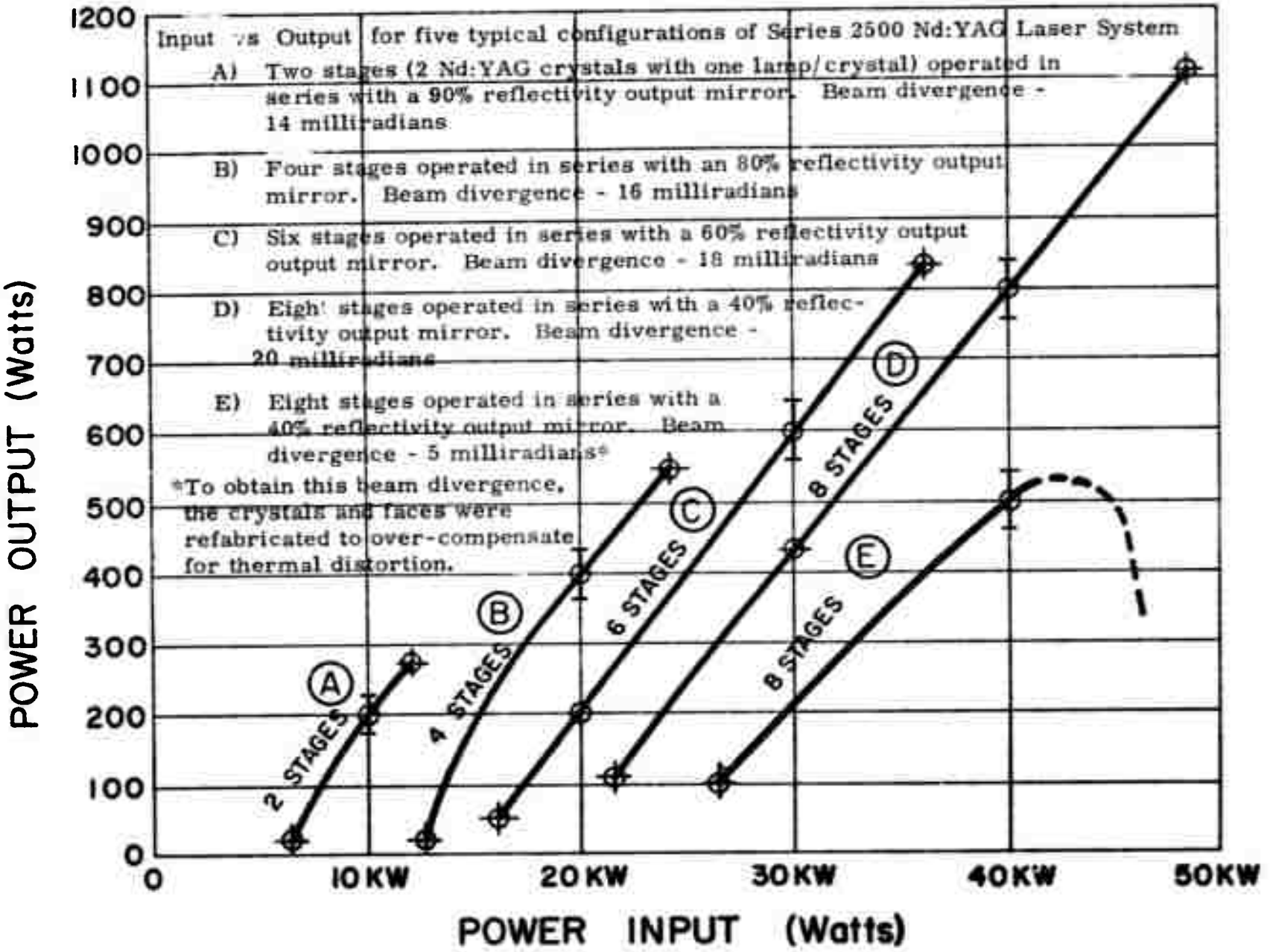

FIGURE 2-1

Output vs Input Curves for Multiple Nd:YAG Laser Heads

consistent with the empirically determined optimum output coupling of 65%. In other words a 35% reflecting output mirror has been found to provide the highest output in the C. W. case. As an additional check on round trip gain, a single surface of a quartz wedge that had been A. R. coated and checked for a reflectivity of less than .2% was used in place of the normal 35% R output mirror and threshold lasing was achieved at 6kW/lamp implying a total round trip gain of greater than 500.

With round trip gains of this magnitude most normal techniques for "Q" switching a C. W. YAG laser such as an acousto-optical cell are inappropriate since the highest depth of modulation achieved in such a device utilizing quartz as the active medium is only on the order of 50%. A mechanical Q-switch is also inappropriate due to the high rotational speeds that would be required. We therefore decided that a Pockels cell was the only way we could achieve the switching times, repetition rates and depths of modulation necessary, and we have in fact devised a means to accomplish this.

Figure 2-2 depicts schematically the method utilized to separate one of the states of polarization. Item A is the end of the last rod in the laser system. Item B is a 90° polarizing prism oriented in such a way that the hypotenuse of the right triangle shown is at 18° to the optic axis through the laser. Item C is a 100% reflecting mirror at 1.06 microns and is placed normal to the reflected beam.

Surface "A" of the prism has been multi-layer coated for an "S" wave reflectivity of 73% at 18° to the optical axis and a "P" wave transmission in excess of 99%. This means, that portion of the beam which is reflected is essentially totally polarized. The output beam exits through the prism and is within a few degrees of normal to the exiting surface so that an A. R. coating is used effectively on that surface as well as on the third surface. Let us consider an unpolarized beam exiting from the laser rod. As the beam strikes the polarizing surface, that portion which corresponds in polarity to the "P" wave passes through the prism without loss. This power represents 50% of the total available. That portion of the beam which corresponds to the "S" wave is split by the proportion of 27 to 73 so that 27% of the S wave passes through the prism also. Therefore a total of 63½%, which, again, is totally

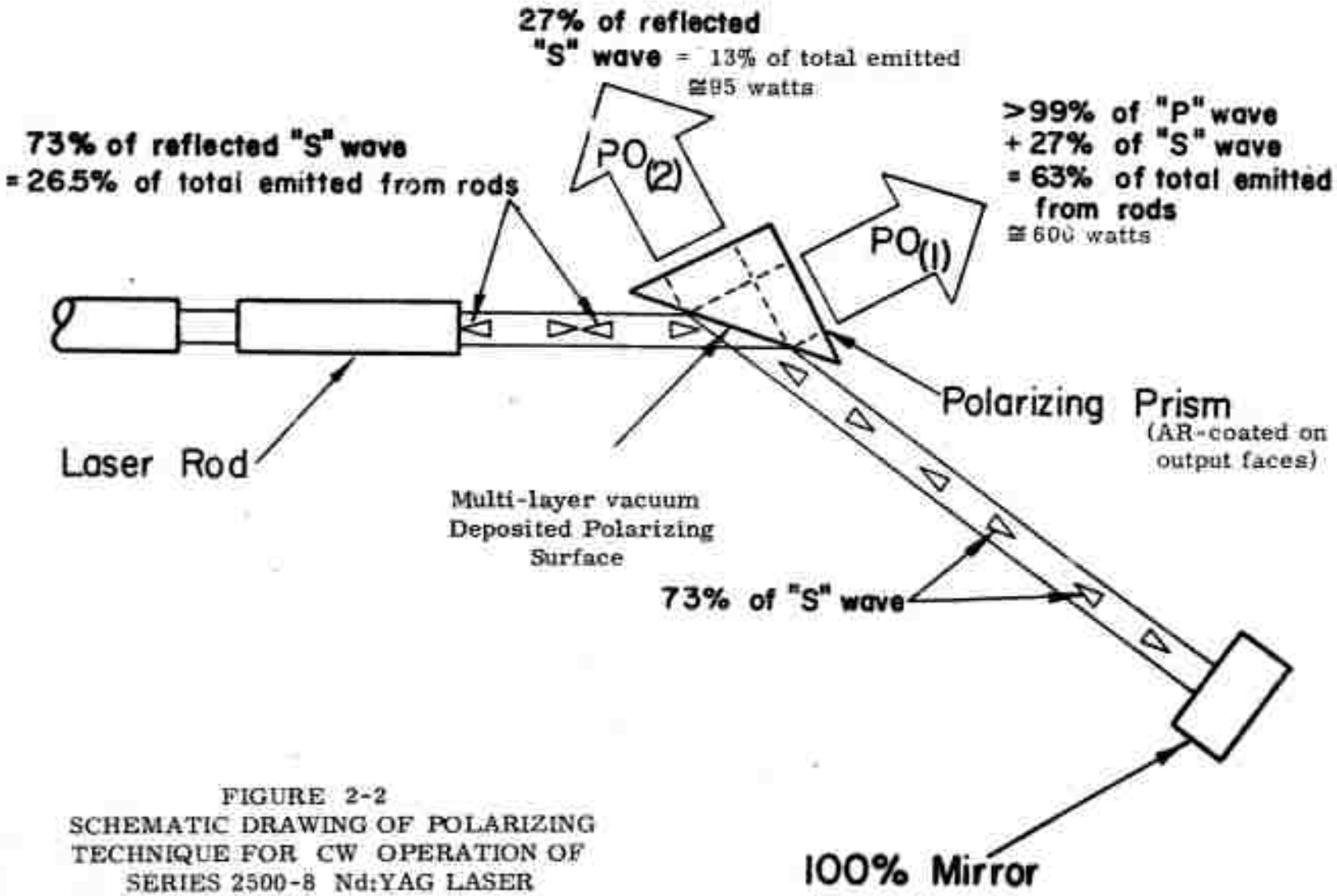

FIGURE 2-2
SCHEMATIC DRAWING OF POLARIZING
TECHNIQUE FOR CW OPERATION OF
SERIES 2500-8 Nd:YAG LASER

polarized in the S direction, is reflected from the 100% mirror and directed back to the polarizer, at which point 27% passes through the polarizer and 73% is reflected back into the laser. This 73% represents only about $26\frac{1}{2}\%$ or in other words 73% of $36\frac{1}{2}\%$ of the total power emitted originally. Therefore the laser effectively has an output mirror reflectivity of only $26\frac{1}{2}\%$. Now, to recap the distribution of power in this device, assume a total umpolarized power emitted from the end of the rod of 1,000 watts, Six hundred thirty-five watts will be emitted in the primary beam (Po_1), 98.6 watts will be emitted in the secondary beam (Po_2) and 266.4 watts will be returned to the laser. All of this 266 watts is polarized in the S wave direction as it initially enters the laser rods. However as the beam passes through the rods and is amplified it encounters strong birefringence and by the time it has made the complete round trip through the laser, the beam polarity is again totally scrambed or unpolarized and at a power level equal to the original 1,000 watts. In operation we have observed slightly over 600 watts C. W. out in the primary beam (Po_1) and 95 watts out in the secondary beam (Po_2) at normal input power. If we block the S wave leg of the split beam the laser stops emitting since there is no reflecting surface normal to the beam. Therefore if we place a second polarizer oriented in such a way as to create a crossed polarizer condition in the S wave leg, we also completely stop the system from lasing. We now have an ideal situation for inserting a Pockels cell between the crossed polarizers. If we operate the cell in the pulse voltage on condition, in other words if we apply a half-wave voltage to the cell, the system will lase.

Figure 2-3 shows the apparatus used to accomplish "Q" switching using this technique. The letter A denotes the prism, the letter B denotes the Pockels cell, C is the second polarizer (a coated plate), D is the 100% reflecting mirror, $Po_{(1)}$ is the primary output beam and $Po_{(2)}$ is the secondary output beam.

A single surface polarizer was obtained from Valpey Corporation which utilized a multilayer dielectric coating to provide a separation of the two states of polarization intracavity. The polarizer is basically a 90° quartz prism with the polarizing surface applied on the hypotenuse. The other two surfaces are A.R. coated for 1.06 microns since a beam is emitted from both surfaces. The prism must be set in the system at an angle of incidence of 72° with respect to the optical axis through the

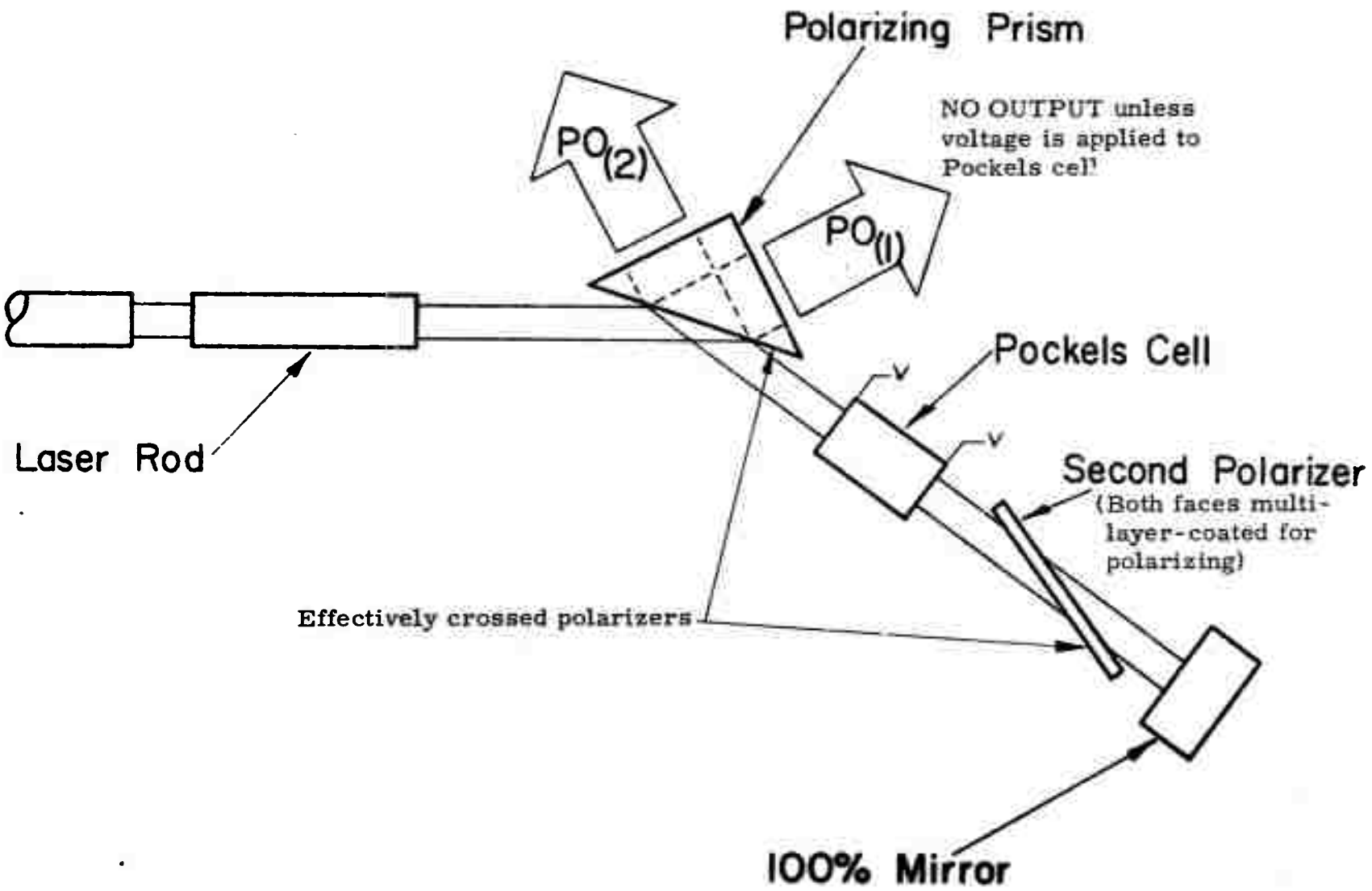

FIGURE 2-3

SCHEMATIC DRAWING OF "Q" SWITCHING TECHNIQUE

laser. A single max reflectivity mirror was aligned with the reflected beam. The characteristics of the polarizer are such that only 36% of the total power incident on the polarizer is reflected, although 99% of this reflected power is polarized. The remainder exits from the prism as the primary output beam.

After the reflected beam strikes the max R mirror it is returned to the polarizer again at which point 73% is reflected back into the laser. (The other 27% exits from the laser as a secondary beam). This means that the effective output reflectivity is only 27%. For maximum CW output this reflectivity should be on the order of 40%. The beam that is returned to the laser is totally polarized; however, by the time the beam has made the round trip through the rods and consequently gained in power, the returned beam is totally unpolarized due to the thermally induced birefringence typical of CW pumped Nd:YAG. Therefore, as the beam reaches the polarizer it is again split with only a part of one polarity reflected so that 36% of the total goes to the mirror which of course starts the process all over again. The primary output beam passes through the polarizer and has two linearly polarized components. The vertical component contains 82% of the total power out. Since the low signal gain of the laser is very high, on the order of 250 times round trip, there is no need for an output mirror.

In operation, the polarizer has shown no tendency to damage. At 5kW input to each lamp, an output power of 600 watts has been observed in the main beam 82% vertically polarized. The secondary beam has been measured at up to 90 watts horizontally polarized and in operation is discarded.

Since there is no real output mirror but instead a polarized beam reflected off the surface of the polarizer and incident on a max reflectivity mirror, a second polarizer is placed in this leg and oriented so that it is crossed with respect to the first polarizer. This of course cuts the laser off since there is no feedback mechanism. However, a Pockels cell placed between the crossed polarizers with a half wave voltage applied does allow the system to lase, thereby allowing the system to be Q-switched. (See Fig. 2-3). In practice a 12kW positive pulse having a rise time of 30ns and lasting for approximately 1 microsecond is applied. The first Pockels cell utilized a KD*P

crystal immersed in trichloroethylene. The output pulses (see Figure 2-4) has a modulation superimposed on the main pulse and had an energy per pulse of 120mJ. The pulse widths were on the order of 30ns for a peak power on the order of 4MW. The repetition rate was increased to 600 pps at which point the fluid in the area of the beam and at the surface of the KD*P crystal began boiling. After replacing this fluid with a Dow Corning silicon oil (DC 200-5) and replacing windows the system operated well at up to 200 pps, however it was obvious that the fluid immersion technique would not be useful at high repetition rates due to heating. In addition it was found that the Pockels cell pulse electronics was inadequate in terms of pulse rise time, voltage capability and repetition rate since all three items degraded at repetition rates in excess of 800 pps.

In the course of measuring the pulse output characteristics it was realized that the modulation seen on the pulse was in fact quasi-self mode-locked with a natural frequency of 77 MHz which corresponds to the c/2L mode of the laser system.

2.2 Mode-Locked Injection Technique

In order to obtain maximum second harmonic generation efficiency with the smallest possible crystal size it is desirable to increase the peak power output of the system to as high a level as possible. The technique which we have proposed and incorporated has demonstrated theoretically and experimentally that substantial increases in peak power can be achieved.

2.2.1 Mode-Locked Injection System Description

The peak power enhancement technique makes use of a continuous mode-locked Nd:YAG laser as a source of very short pulses which are injected into the cavity of the main high power laser, acting as seed pulses from which the Q-switched output can grow rather than from the natural laser fluorescence. The pulse injection is accomplished by sharing the output mirror of the CW mode-locked system with the front termination reflector for the main laser, as diagrammed in Figure 2-5 .

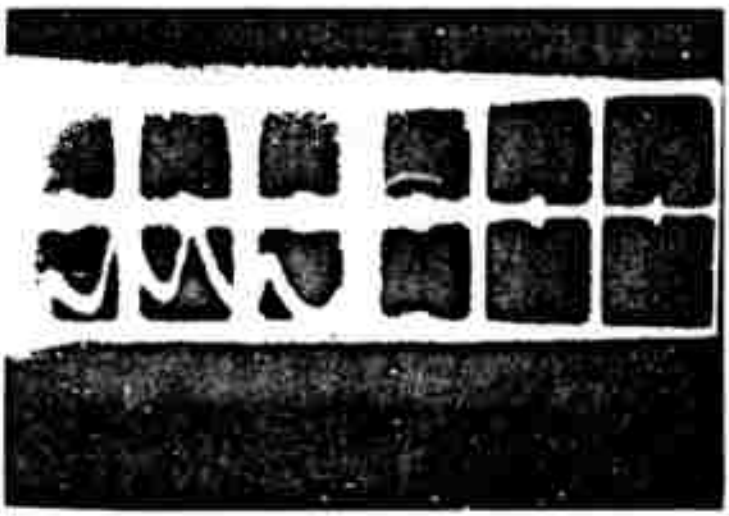

FIGURE 2-4

SINGLE TRACE OF Q-SWITCHED OUTPUT FROM SERIES 2500 8-STAGE LASER SYSTEM SHOWING TYPICAL SELF-MODE-LOCKING TENDENCY AT 77 MHz

HORIZONTAL SCALE - 20 NANOSECONDS/DIVISION
VERTICAL SCALE (APPROX.) - 5MW/DIVISION
TOTAL ENERGY = 150 MILLIJOULES

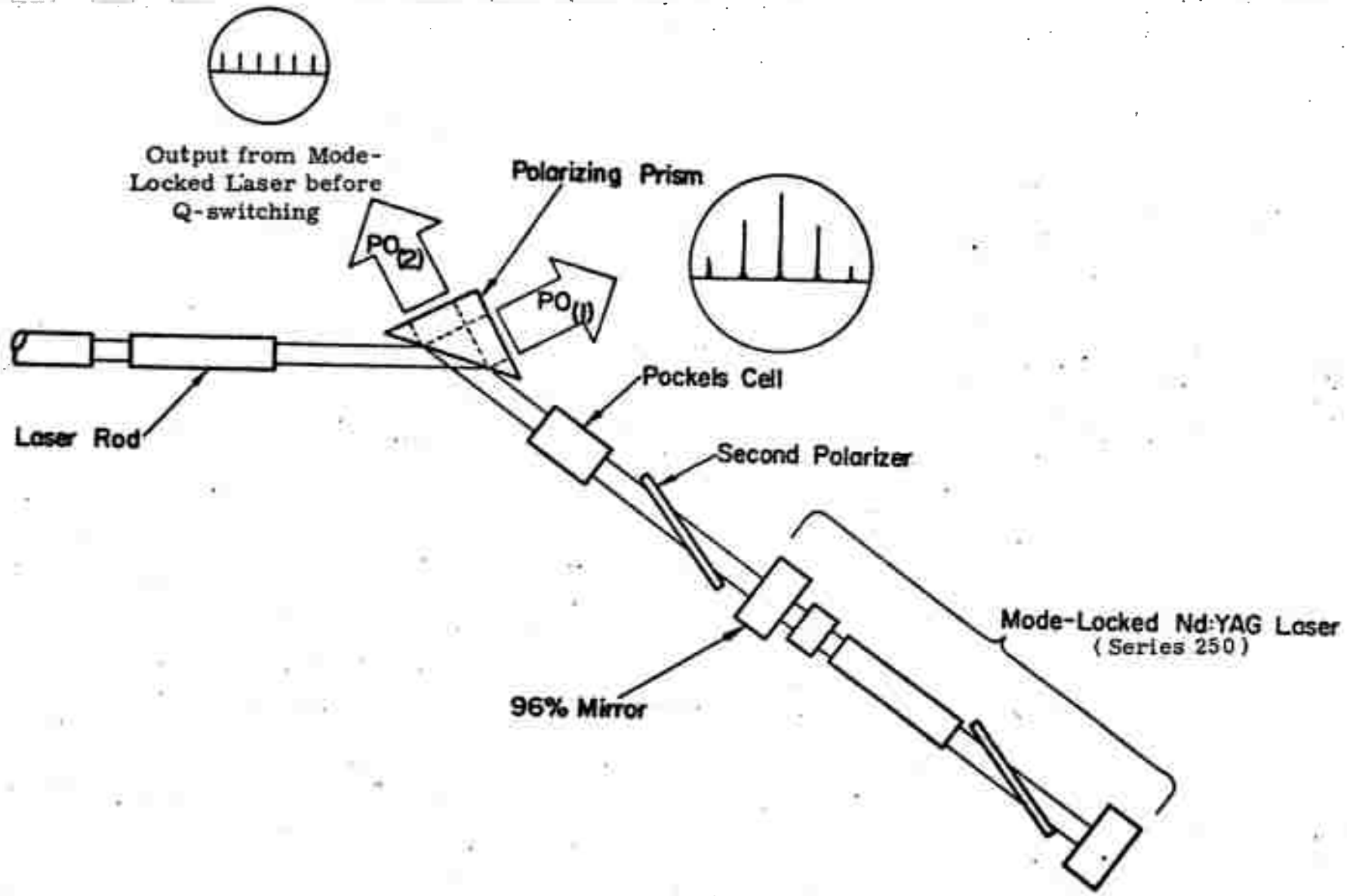

FIGURE 2-5

DETAIL SCHEMATIC OF SERIES 250 MODE-LOCKED LASER PROVIDING "SEED" PULSES TO SERIES 2500 8-STAGE Q-SWITCHED LASER SYSTEM

A compromise reflectivity between the 90% optimum for the mode-locked system and 100% optimum for the main laser is utilized. With no voltage applied to the Pockels cell the horizontally polarized beam from the mode-locked system passes through the prism polarizer with a negligible portion (less than 1%) reflected into the high power system. In the ideal circumstance in which the Pockels cell is switched rapidly, in a time short compared with the time between mode-locked pulses, and with perfect synchronization one mode-locked pulse with a width of less than 200 picoseconds and an energy of approximately 3×10^{-8} joules is injected. If this amount of energy is adequate to completely dominate the natural fluorescence of the system, a condition which is met in practice, the Q-switch laser pulse will emerge with an energy essentially identical to that for the pure Q-switched condition but having the form of a pulse train consisting of narrow pulses separated in time by the round trip transit time of the main laser. An actual pulse photograph is shown in Figure 2-6 . The envelope of this pulse train has a width approximately equal to the pure Q-switched pulse. Neglecting saturation, the second harmonic generation process can be enhanced by factors of greater than 10 to 1 by this technique. Our system has demonstrated a 5 to 1 ratio, the discrepency being due previously to the imperfect electronic switching. In the implementation of this technique we have made use of both an open loop and a closed loop CW mode-locking system operating at 77 MHz, coincident with the round trip transit frequency of the main laser. The mode-locking system utilizes phase modulation, accomplished by means of a barium sodium niobate crystal, with electronics circuitry to provide closed-loop control of the modulator driving frequency so as to maintain perfect synchronization with the laser cavity frequency. A description of the closed loop mode-locking system developed independently by Holobeam, Inc. can be found in the appendix.

HORIZONTAL SCALE
20 N.S./DIV

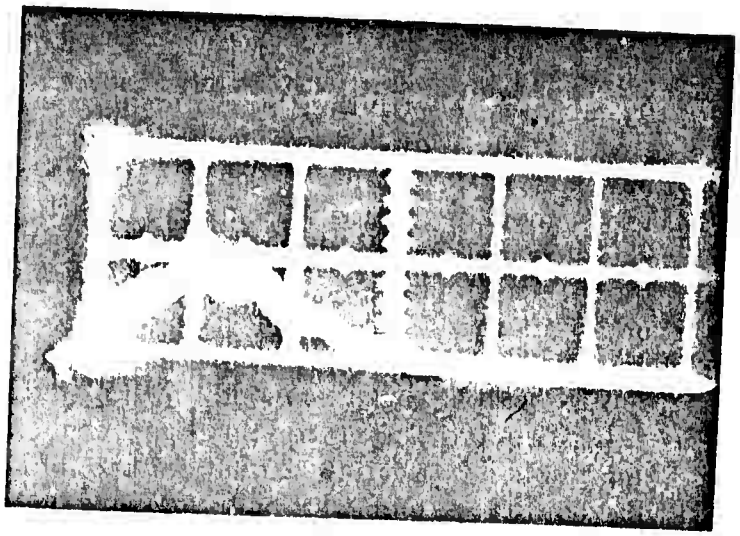

"Q" SWITCHED ONLY

NOT REPRODUCIBLE

HORIZONTAL SCALE
13 NS BETWEEN
PULSES

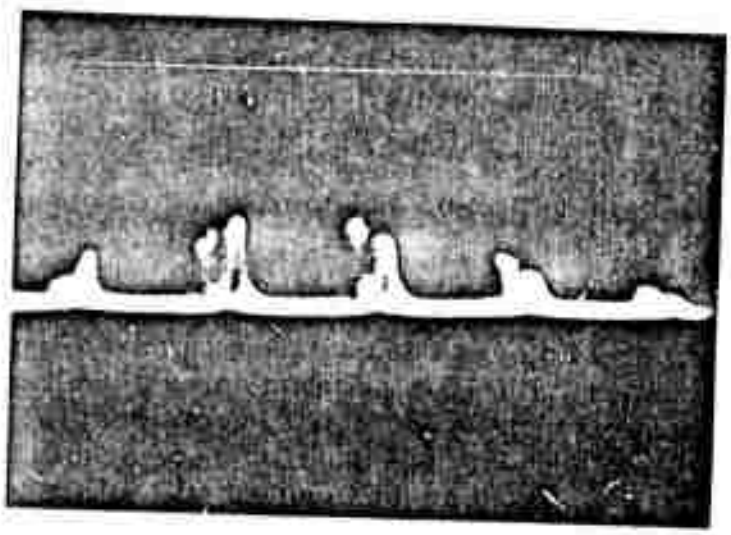

"Q" SWITCHED AND MODE LOCKED

MULTIPLE TRACES SHOWING DIFFERENCE BETWEEN NORMAL "Q SWITCHED OUTPUT AND "Q" SWITCHED WITH OPEN LOOP MODE LOCKING OUTPUT AT EQUAL ENERGY PER PULSE

FIGURE 2-6

2.2.2 Experimental Results

The closed loop mode-locking electronics was completed and tests indicated that an output of 2 watts stably mode-locked at 77MHz could be obtained. The Series 250 complete mode-lock system was installed parallel to the Series 2500-8 stage laser according to the diagram in Figure 2-7 . After resolving some coating problems with quartz windows obtained from Isomet Corp. a dry Pockels cell was designed and constructed utilizing highly deuterated KD*P obtained from Isomet since tests had shown this material could withstand in excess of 800 watts CW without overheating. In operation it was found that although there was some feedback from the Q-switched laser, the closed loop mode-lock system could mode-lock the Q-switched pulses reliably at repetition rates of up to 1000 pps. However the pulse energy fell off above 800 pps due to lower pulse voltages on the Pockels cell above that rate The output energy per pulse was maintained at between 100 and 110 mJ (see Figure2-8), however the pulse envelope width was somewhat longer during mode-lock operation possibly due to a slow rise time on the voltage pulse to the Pockels cell.

2.3 Switching Electronics

In order to produce optimum mode-locked pulse injection the Pockels cell should switch in a time short compared with the pulse-pulse separation and at a time accurately synchronized with the mode-locked pulse train. The thyratron pulses used in our initial experiments were borrowed from our low power CW laser system and had a switching time of approximately 30 nanoseconds. No synchronization was possible. In spite of this we could obtain stable mode-locked enhanced second harmonic generation. However, the observed 5:1 enhancement ratio was a factor of three worse than we should be able to achieve. We believe that this is due to incomplete injection, the mode-locked pulse being unable to dominate the fluorescence from the high power amplifier.

We have made some attempts to improve the switching speed of the electronics by using a different thyratron and better circuitry but have not tried the new switch in our SHG experiments.

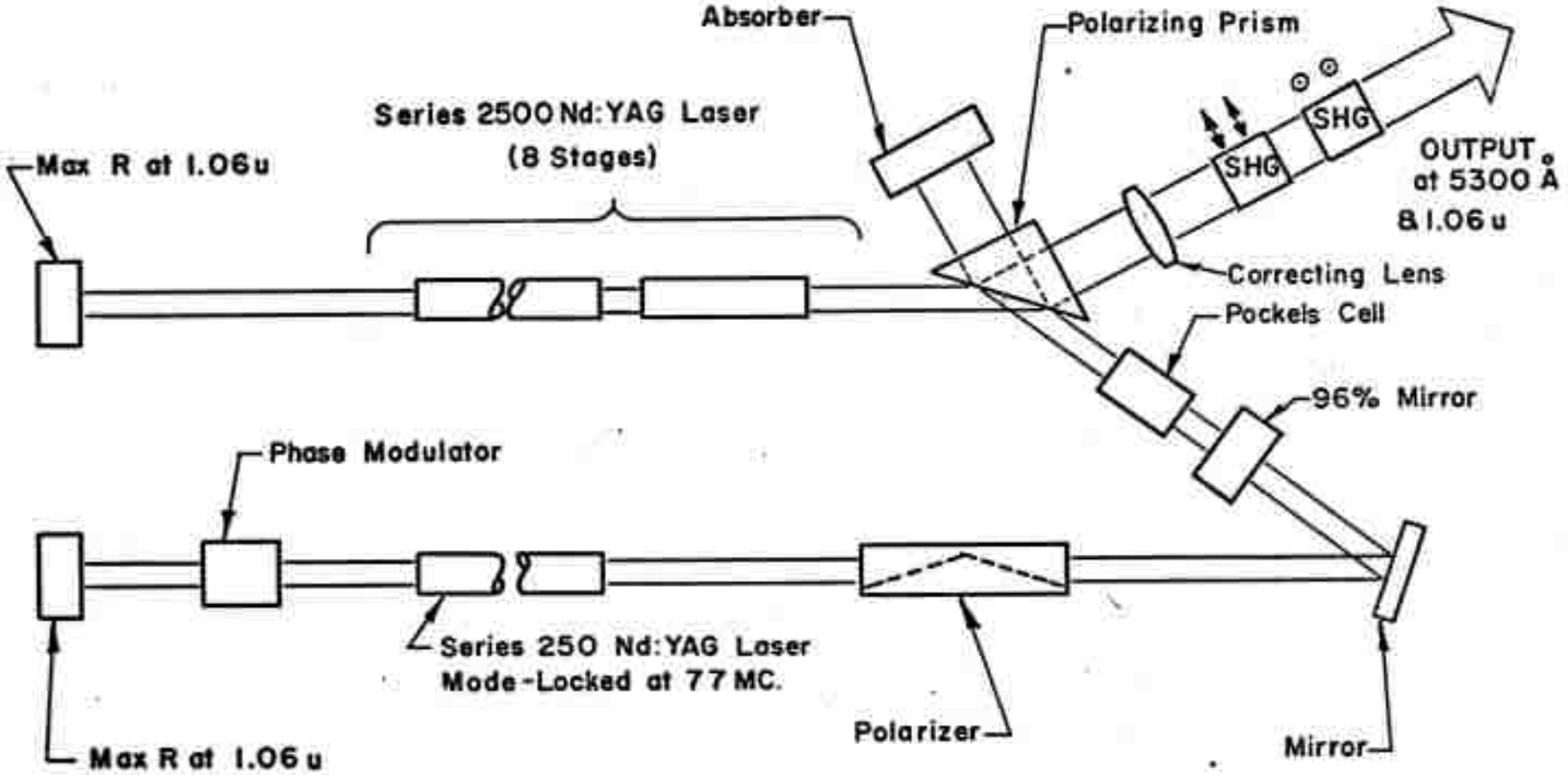

FIGURE 2-7

DETAIL SCHEMATIC OF COMPLETE Q-SWITCHED AND MODE-LOCKED AND FREQUENCY-DOUBLED SERIES 2500 8-STAGE LASER SYSTEM

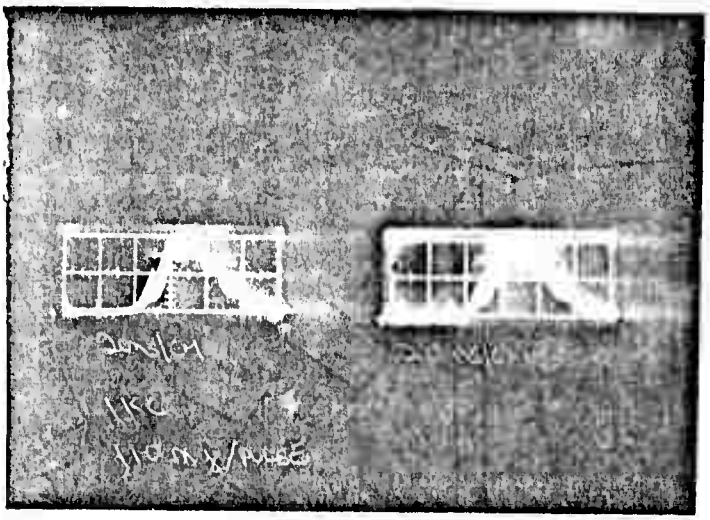

HORIZ. SCALE=
20NS/DIV
VERT. SCALE=
2.5MW/DIV

TYPICAL "Q" SWITCHED PULSES AT 1000 P.P.S.
AND 110 WATTS AVERAGE OUTPUT POWER UTILIZING
HOLOBEAM DESIGNED DRY POCKELS CELL "Q" SWITCH

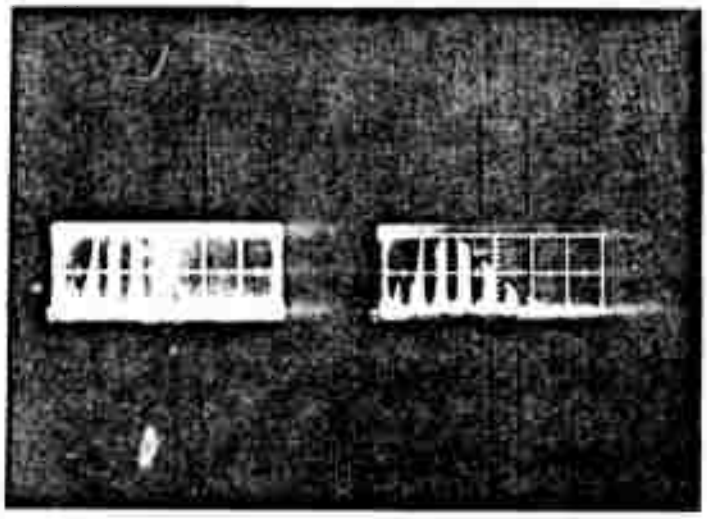

HORIZ. SCALE=
20NS/DIV
VERT. SCALE=
25MW/DIV

FIGURE 2-8

SAME AS ABOVE WHEN CLOSED LOOP MODE-LOCKING INITIATED

OSCILLOSCOPE TRACES OF CLOSED LOOP MODE-
LOCKED "Q" SWITCHED
OUTPUT AT 110 M.J./PULSE

SECTION III

NON-LINEAR MATERIALS

One of the major areas of concern in this program has been the selection and optimum utilization of a non-linear material which will yield high conversion efficiencies at high average powers from a multi-transverse mode laser.

3.1 Nonlinear Crystal Survey:

Since we recognized at the onset of the program that any non-linear crystal used to generate the 0.533 micron second harmonic of the 1.065 micron laser fundamental in Nd:YAG must be optically transparent at both wavelengths, many materials were precluded as primary candidates. As the program proceeded, only those non-linear crystals showing less than one percent absorption at 1.065 per centimeter were considered. Our own special technique for measuring 1.065 absorption (as described in paragraph 3.2) was utilized in making this selection. From materials so tested, only five major choices remained which showed less than 1.% cm^{-1}. Since both peak and average power levels encountered by these crystals are highest at 1.065 microns, the selection of nonlinear materials for use in our experiments was predicated upon lowest absorption at that wavelength, with secondary emphasis placed upon their absorption at the second harmonic.

Listed below in Table I, are the five materials which were given serious consideration in order of their degree of nonlinearity.

TABLE I

NONLINEAR CRYSTAL SELECTION

MATERIAL	POINT GROUP	LARGEST NONLINEAR COEFFICIENT (*)	PHASE-MAT ANGLE AND TEMPERATU
$Ba_2Na\ Nb_5O_{15}$	mm2	$d_{32} = 41. \pm 4.$	90^o @ 105^oC
$LiNbO_3$	3m	$d_{31} = 14. \pm 2.$	90^o @ 165^oC
$LiIO_3$	6	$d_{31} = 11. \pm 2$	$29^o50'$ @ 25^oC
KD_2PO_4	42m	$d_{36} = 1.0 \pm 0.1$	$39^o57'$ @ 25^oC
CsD_2AsO_4	42m	$d_{36} = 0.55 \pm 0.05$(1)	90^o @ 101 ^oC

(*) relative to d_{36} for KD_2PO_4

(1) Measured valve may be in error due to improper crystal growth.

Thus far, CsD_2AsO_4 has given us the highest overall conversion of 1.065 micron output into average 0.533 micron second harmonic power. This is somewhat peculiar, since it has the smallest degree of nonlinearity of all materials listed above. The two major factors which limit SHG conversion efficiency in $Ba_2NaNb_5O_{15}$ and $LiNbO_3$ are thermal runaway due to the poorly understood nonlinear heating effect at phase match, and the nonlinear catastrophic damage phenomenon, also poorly understood. Both $LiIO_3$ and KD_2PO_4 are limited by the large angular walkoff between the second harmonic and fundamental Poynting vectors, precluding the efficient use of long crystals. Essentially CsD_2AsO_4 is the only remaining choice which combines the advantage of 90-degree phase-matching angle and inherently greater angular acceptance with minimal self-heating due to nonlinear thermal effects. Curiously at high power levels actual SHG conversion efficiencies observed in these materials have varied roughly inversely, rather than directly with the magnitude of their nonlinear coefficients.

3.2 Optical Absorption Measurement

In our past experience we have found very few optical materials that have withstood average 1.065 micron power densities beyond 25 kilowatts/cm^2 when placed in the high power output beam of our CW Nd:YAG system. Fused silica, undoped YAG and diamond are the only materials which have shown little or no lensing effect due to thermally-induced refractive index distortion at this wavelength. All other materials, including all nonlinear crystals tested, have shown significant thermal lensing. Therefore it became imperative to develop a technique for measuring relatively small residual absorption in nonlinear crystals, first to determine whether they would survive high average power levels at 1.065 microns, and secondly to aid in predicting the degree of phase mismatch resulting from thermally-induced nonuniformity across the input beam diameter. For this purpose we developed a successful technique based upon balancing the heat generated within a polished crystalline sample with a known amount of cooling developed by a Peltier junction device held in intimate contact with the crystal under

vacuum conditions such that no other heat loss by convection took place.

The actual construction of the Peltier device is shown in the accompanying photograph, Figure 3-1 & 3-2.The base is machined from a special aluminum extrusion which clamps to our standard optical rail, and also serves as the hot junction heat sink for the Peltier cooler. The thermoelectric element itself consists of a doubly cascaded pair of semiconductor elements sandwiched between two aluminum plates and is configured to provide uniformity of temperature across the top cold junction plate. The unit was purchased from the Cambridge Thermionic Corporation as their Model 3955-1, which was selected for efficient operation at low current input levels, and because the top surface dimension of 1/2 inch coincided with the approximate side face dimensions of most crystals tested. The outer case is sealed with vacuum-tight fittings and incorporates an opposite pair of doubly antireflection-coated fused silica windows centered with respect to the axis of our Series 250 CW Nd:YAG system. A vacuum exhaust port permits hookup to a vacuum pump through a vacuum needle valve and liquid nitrogen cold trap. Additional vacuum sealed electrical feed through connections are provided to the Peltier cooler and to internal calibration terminals. A teflon shroud is placed beneath the top plate of the cooler for extra stray light shielding, and a gold-plated copper plate is placed atop the cooler to reflect away any spurious scattered light from the surfaces of the crystal under examination. A pair of Yellow Springs Instruments Corp. #44005 thermistor beads were used to record thermal equilibrium by inserting one at the top plate of the Peltier cooler in a drop of Wakefield Engineering Corp. zinc oxide impregnated silicone grease and the other into a hole drilled into the bottom aluminum block. A sensitive mercury battery driven Wheatstone bridge was used in conjunction with a Keithley Model 150B microvolt-ammeter to record null condition at room temperature.

A first trial run was conducted with a polished 1.0 cm^3 of best quality fused silica. A ten-watt 1.065 micron beam derived from a multimode CW Nd:YAG source was transmitted through

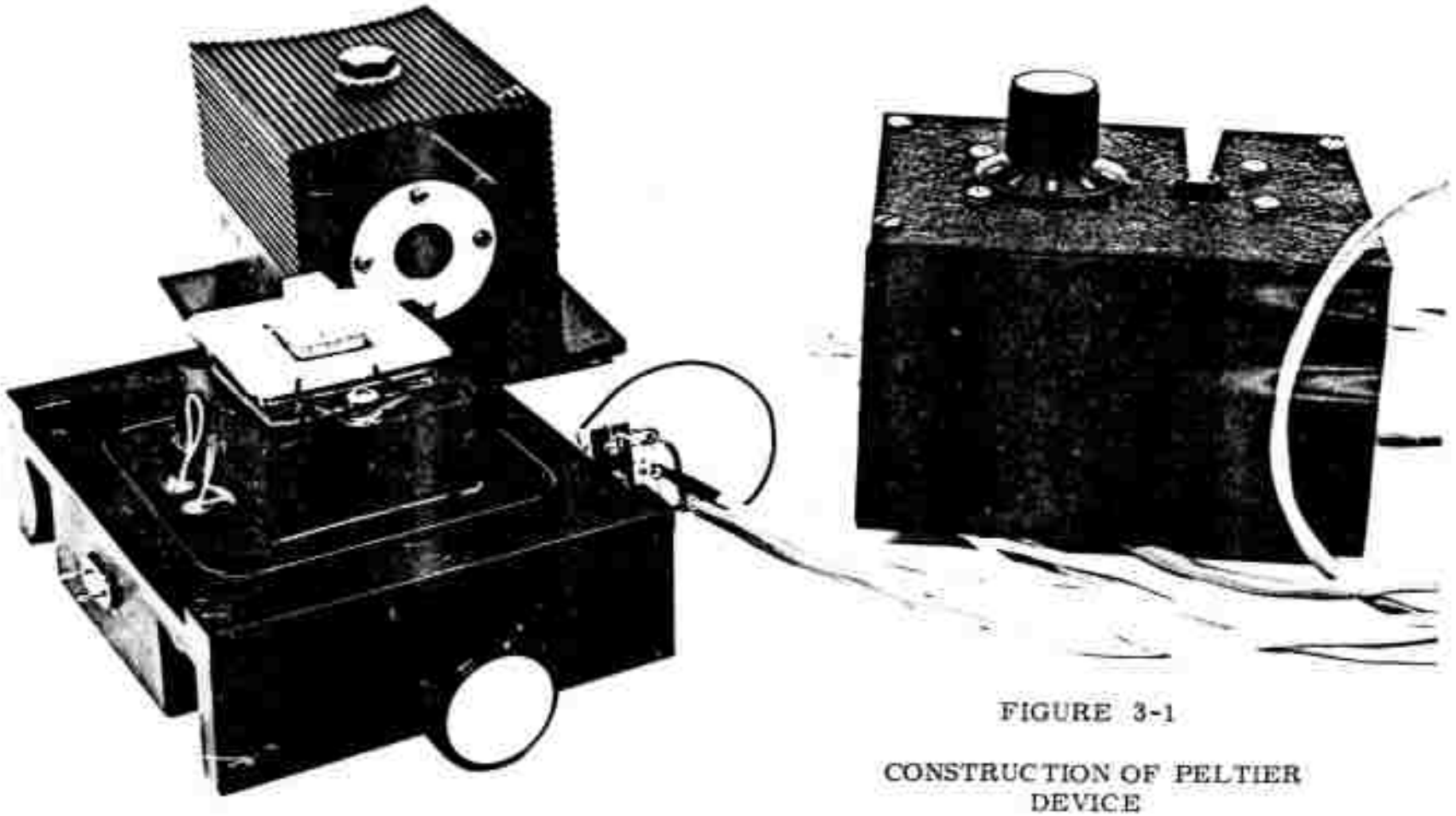

FIGURE 3-1

CONSTRUCTION OF PELTIER DEVICE

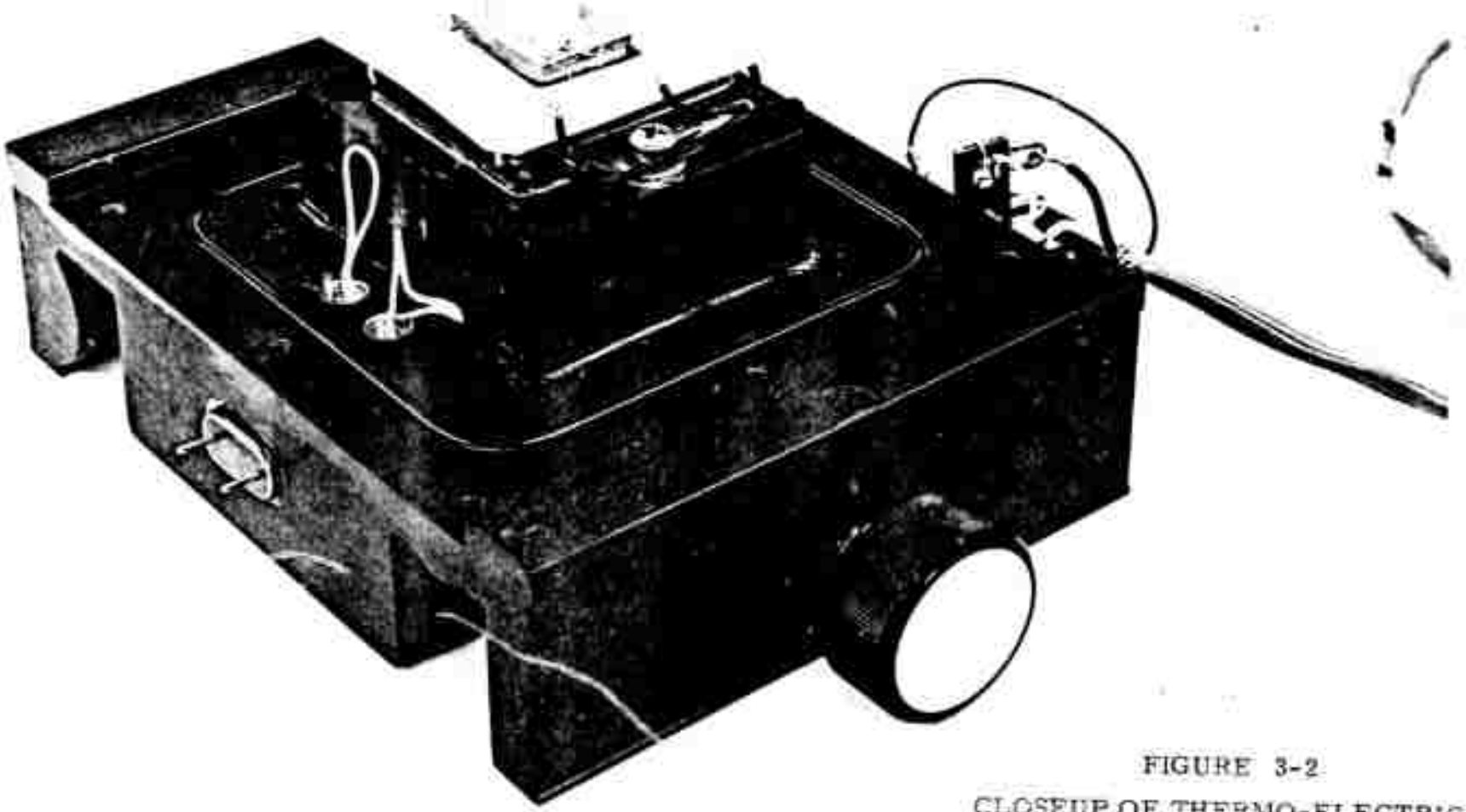

FIGURE 3-2

CLOSEUP OF THERMO-ELECTRIC
COOLER ASSEMBLY

a 1.5 millimeter aperture stop, then through the Peltier cooler assembly evacuated to less than 10^{-5} mm. Hg., which contained the sample. The exit beam was captured by a Coherent Radiation Labs. Model 201 CW power meter, and the laser was peaked to provide 10.0 watts. The Keithley microvolt-ammeter was quickly driven off-scale by absorption within the SiO_2 block. A small amount of current was then fed to the Peltier cooler to re-establish the previously set null point on the microvoltmeter. It was found that 3.6 milliamps of cooler current restored null, and that adequate sensitivity could be maintained at other laser power input settings using SiO_2 as a low absorption check.

A full calibration of the Peltier cooler under 10^{-5} mm Hg vacuum conditions was then made utilizing a specially prepared aluminum block with a 100-ohm carbon resistor embedded within it. Heat, measured as the I^2R loss to the calibration resistor, was offset by the Peltier cooler current, and the calibration curves shown in Figure 3-3 were recorded for the three different Simpson milliameter ranges used in later measurements.

Subsequent tests were performed on several specimens of nonlinear crystalline materials. Table II shows a complete list of test results obtained with a transmitted power at 1.065 microns of 10.0 watts under identical conditions. After each crystal was examined for its total heating effect upon the gold-plated copper plate, a teflon spacer ring was inserted under the crystal to thermally isolate it from the Peltier cooler. A second run was then made under vacuum conditions to ascertain what fraction of the total heating effect was due to combined internal Tyndal scattering and residual scattering from the polished crystal aperture faces. This contribution due to scattering was then subtracted from the original total heating term to yield a net figure for the absorption of a given length sample. The last column in Table II shows the re-normalized absorption for each sample per centimeter length.

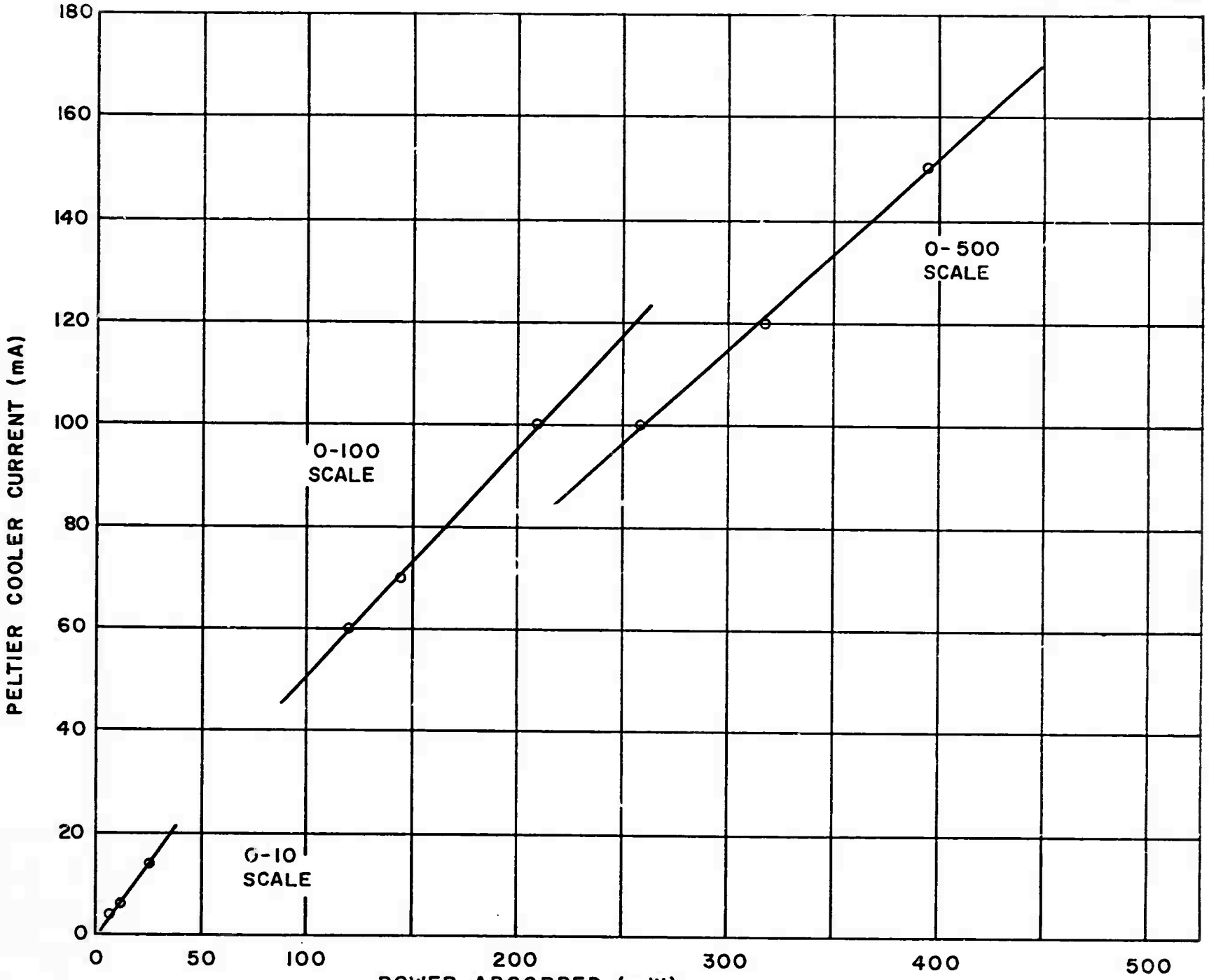

PELTIER COOLER CALIBRATION CURVE

TABLE II

PERCENTAGE ABSORPTION PER CENTIMETER OF LENGTH
FOR NONLINEAR CRYSTAL SPECIMENS

Crystalling Material	Crystal Length (mm)	Null Current to Peltier Cooler, (10W Laser Input) (mA)	Cooling Power from Calib. Curve (mW)	Correction Due to Scattering (mW)	Adjusted Value for Absorption (mW)	Percentage Absorption per Centimeter crystal Length
CsD_2AsO_4	12.0	70.	155.	42.	113.	0.94
CsD_2AsO_4	10.0	60.	134.	36.	98.	0.98
CsH_2AsO_4	15.5	225.	610.	50.	560.	3.6
CsH_2AsO_4	15.5	215.	580.	50.	530.	3.4
KD_2PO_4	12.5	38.	95.	11.	84.	0.67
KD_2PO_4	12.5	41.	98.	11.	87.	0.70
KD_2PO_4	19.2	41.	98.	10.	88.	0.46
$LiIO_3$	5.0	6.5	11.	1.	10.	0.20
KH_2PO_4	14.0	450.	1040.	62.	978.	7.0
$Ba_2NaNb_5O_{15}$	5.0	9.3	16.0	1.	15.0	0.30
$Ba_2NaNb_5O_{15}$	5.0	8.9	15.4	1.	14.4	0.29
SiO_2 Block (as reference)	10.0	3.6	6.1	- - -	6.1	0.06

TABLE III

AVERAGED PERCENTAGE ABSORPTION FOR NONLINEAR CRYSTALS TESTED.

Crystalline Material	Chemical Symbol	Measured Average Absorption per Centimeter
Lithium Iodate	$LiIO_3$	0.0020 ± 0.0001
Barium Sodium Niobate	$Ba_2NaNb_5O_{15}$	0.0030 ± 0.0001
Deuterated KD*P	KD_2PO_4	0.0061 ± 0.0012
Deuterated CD*A	CsD_2AsO_4	0.0096 ± 0.0002
Ordinary CDA	CsH_2AsO_4	0.035 ± 0.001
Ordinary KDP	KH_2PO_4	0.070 ± 0.002
Fused Silica (as reference)	SiO_2	0.0006 ± 0.0001

TableIII is a consolidated listing of percentage absorption per centimeter length averaged over one or more measured specimens for each nonlinear crystal tested. With the exception of KD_2PO_4, the average deviation from one sample to another was relatively small. The one sample of KD_2PO_4 which showed significantly lower absorption came from a different vendor than the others and is believed to be of higher deuteration.

3.2.1 Transmission Data

We have taken spectrophotometer tracings of CD*A and KD*P. These are shown in Figure 3-4. Note that the CD*A sample has a measureably larger absorption at 0.355μ (third harmonic of 1.065μ).

3.3 Phase-Match Temperature and Efficiency of the Arsenates

A pulsed Nd:YAG laser was utilized to roughly measure the phase-match temperature and obtain an approximate efficiency. It was also desirable to determine, if possible, a damage threshold level for CDA and CD*A in terms of power density. The laser initially used was a 10 pps 3mm diameter system capable of 3MW peak power. It was found that the phase-match temperature for CD*A was around 97° and very broad — on the order of ±3°C. The efficiency for a power density of 50MW/cm^2 was 12%. The phase-match temperature for CDA was found to be 39.9°C and more critical than in CD*A. The efficiency was essentially the same as CD*A. Since no damage occurred to either crystal it was decided to increase the power density by utilizing a different pulsed YAG laser. This system was capable of an output of 180mJ/pulse operating at up to 5 pps and had a peak power of 20MW in a 5mm diameter beam. For comparison purposes a 2cm long KD*P crystal cut for angular phase matching was utilized for SHG. At a power density of 80mW/cm^2 the KD*P produced an efficiency of 5.4% (beam divergence was on the order of 4mR). At the same power density a 1 cm long CDA crystal was found to have an efficiency of 16% at phase-match temperature. No damage occurred to the crystal so

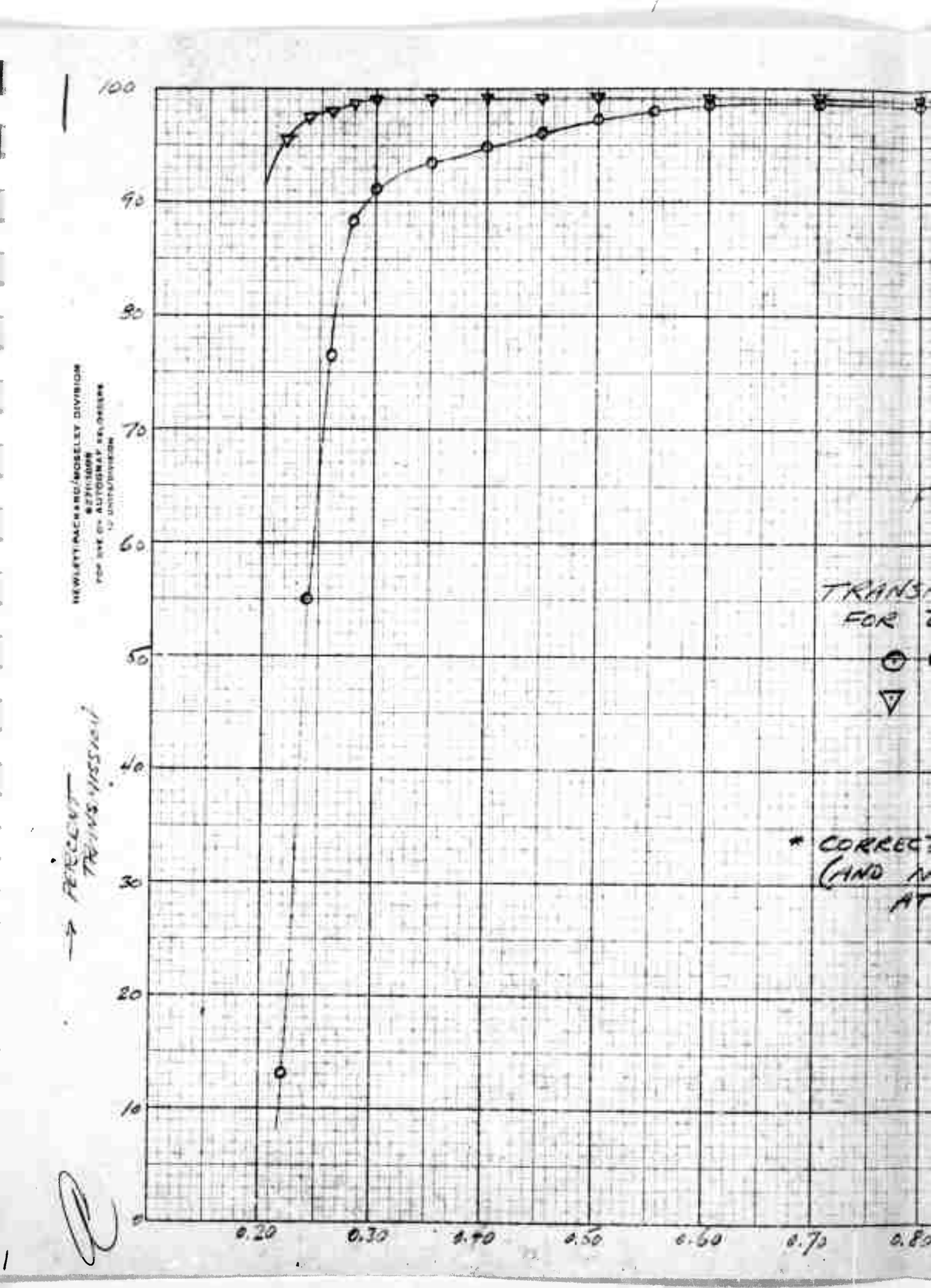
100
90
80
70
60
50
40
30
20
10
0
0.20
0.30
0.40
0.50
0.60
0.70
0.80
PERCENT TRANSMISSION
TRANS
FOR
* CORREC
(AND N
AT

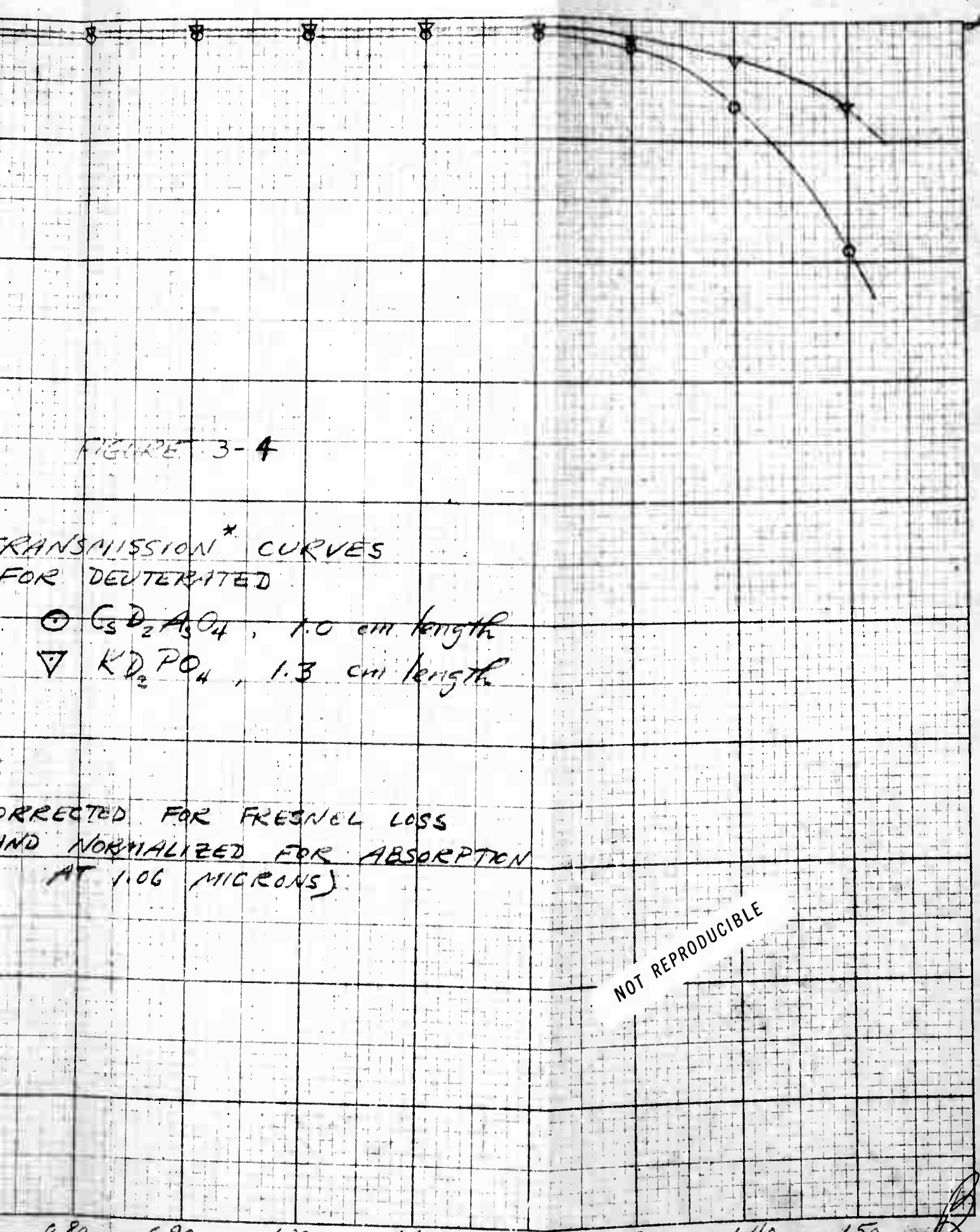

FIGURE 3-4

RANSMISSION* CURVES
FOR DEUTERATED

⊙ $C_5D_2A_5O_4$, 1.0 cm length

▽ KD_2PO_4, 1.3 cm length

ORRECTED FOR FRESNEL LOSS
IND NORMALIZED FOR ABSORPTION
AT 1.06 MICRONS)

the power density was increased by weakly focusing the beam to a diameter of 3mm, yielding a power density of 280MW/cm^2. No damage occurred with the 1.06 micron radiation alone. See Figure 3-5. At phase-match temperature the efficiency increased to 30%. After operating for several minutes at 5pps it was found the fluid used in the cell (DC 200-5) was breaking down but no damage was seen on the CDA crystal, therefore it is concluded that the damage threshold for CDA is in excess of 300mW/cm^2.

3.4 CsD_2AsO_4 Temperature Phase-Matching

Figure 3-6 is a photograph of the oven configuration used to accurately determine the phase-matching characteristics of CsD_2AsO_4 versus temperature. The inner split block was machined from a copper rod of approximately 460 grams mass, and provides uniform heating of frequencydoubling crystals 1.0 centimeter cube in size. A 70-ohm heater winding is situated in the outer housing wound around a copper tube which transmits heat uniformly to the inner copper block. Sufficient teflon insulation is provided between the heater and the outer oven housing to form an adiabatic jacket surrounding the entire copper interior. Doubly antireflection coated fused silica windows are positioned in air-tight seals at each end of the oven assembly. Electrical heating is provided from an automatically proportioning magnetic amplifier which senses the central oven temperature by means of an iron-constantan probe inserted into the split copper block. The overall rate of heating and the maximum oven temperature can be adjusted by proper selection of series ballast resistance.

Figure 3-7 is an actual trace of the temperature phase-matching profile for a 10.5 millimeter length of CsD_2AsO_4 cut for 90-degree phase matching with the input laser signal propagating parallel to the crystalline (110) direction. The trace was produced

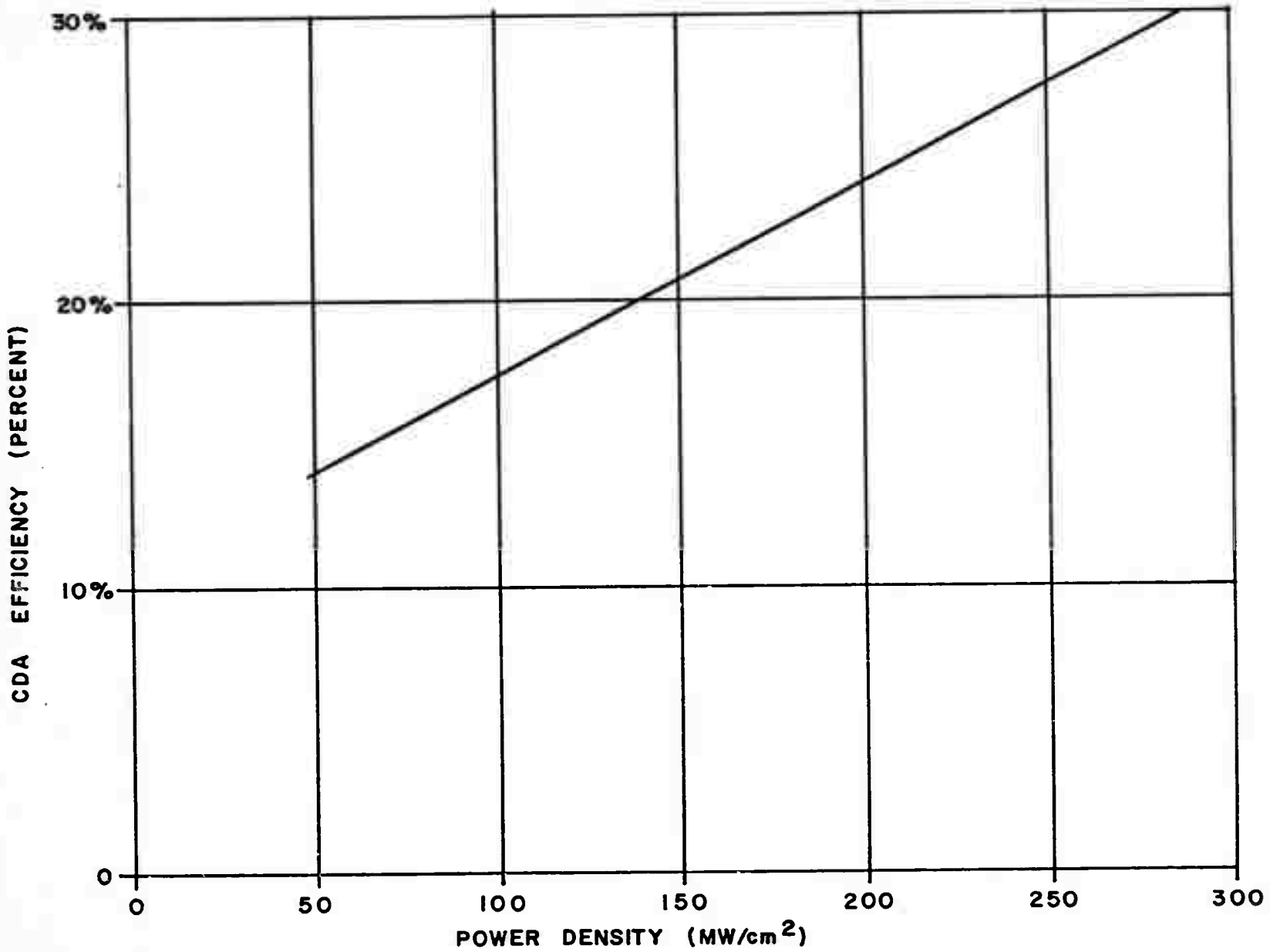

CDA EFFICIENCY VERSUS POWER DENSITY FOR PULSED OPERATION

FIGURE 3-5

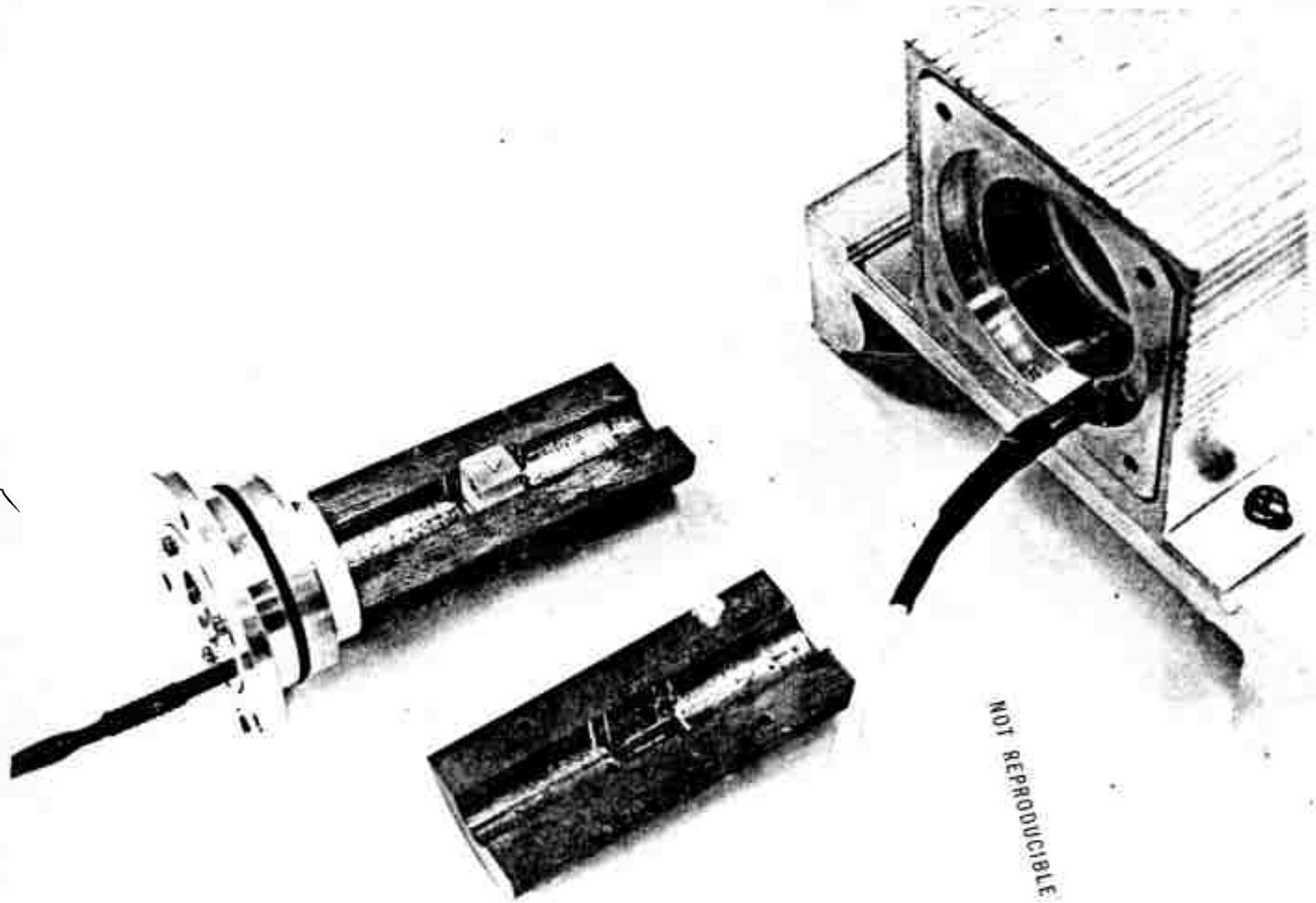

Figure 3-6
Oven assembly for testing phase-match temperature of 90° phase-matchable SHG materials

by first allowing the oven temperature to exceed 130°C, then turning off heater power and letting the crystal slowly cool through its $\sin^2 \frac{(\Delta kl)}{2} / \frac{(\Delta kl)}{2}^2$ maxima and minima while subjected to a half-watt, linearly polarized TEM_{oo} input beam from a CW Nd:YAG laser. An S-4 cathode photomultiplier was provided with a narrow bandpass filter peaked at 0.533 microns, and its anode current fed to a fixed load resistance across the Y-channel input to an X-Y recorder. The X-channel was used to monitor temperature by the output from a microvoltmeter connected directly to the iron-constantan thermocouple imbedded in the crystal oven. Only a course adjustment of CsD_2AsO_4 crystal angle was required with respect to the input laser beam since its angular insensitivity had been verified earlier.

The resultant curve in Figure 3-7 indicates that the CsD_2AsO_4 sample tested has a central peak situated at 101°C, with a half SHG maximum bandwith, $\Delta T_{1/2}$, equal to 5.6°C. Both the position of the central maximum with respect to temperature and the half-power temperature bandwidth are strongly dependent upon the level of deuteration for a given CsD_2AsO_4 sample. It is therefore very important to run an individual check of both these factors for each delivered specimen, especially if two or more crystals are to be used in a tandem frequency doubling arrangement. Conversely, these factors can be utilized as criteria for judging the level of deuteration, which shifts the temperature peak, and the degree of crystalline homogeneity, which should prove directly related to the half-SHG-power temperature bandwidth for a given length sample.

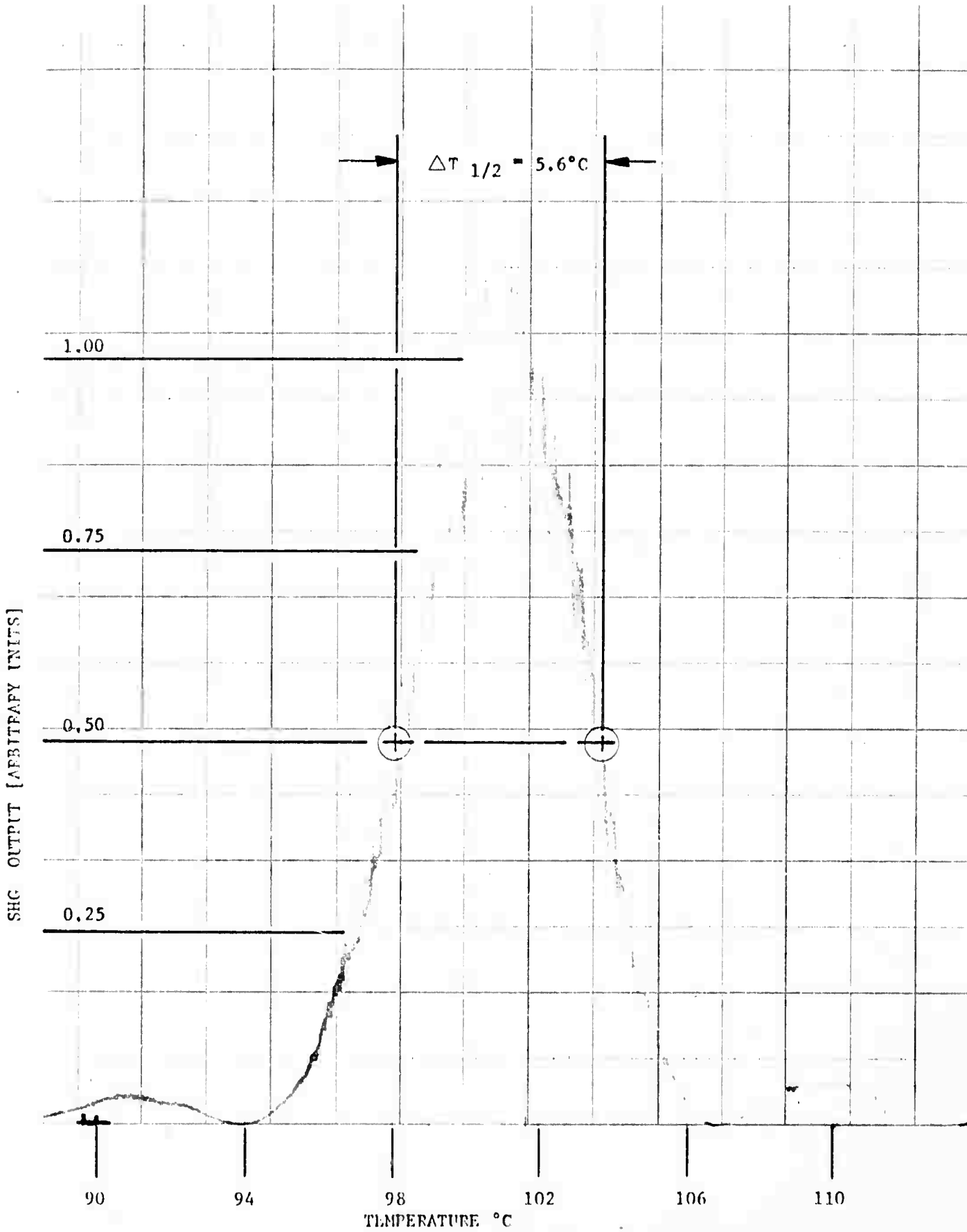

CsD_2AsO_4 PHASE-MATCH VERSUS TEMPERATURE

NOT REPRODUCIBLE

FIGURE 3-7

SECTION IV

SECOND HARMONIC GENERATION AT HIGH AVERAGE POWER

We will first present the experimental evidence in chronological sequence and then discuss the implications of the data with respect to theoretical predictions.

4.1 SHG Apparatus and Tests

The complete system at this point in the development program is shown in Figures 4-1 through 4-6. The SHG oven shown in Figure 4-7 and situated outside the laser cavity is also a vacuum chamber since the CD*A material is very hydroscopic and must be protected against water or water vapor. Two ovens are enclosed in the same chamber since it was expected that multiple crystals would be utilized to obtain maximum output at 0.53μ. The first test at full power allowed only the central portion of the beam to be incident upon the CD*A crystal at a power density of approximately 5mW/cm^2 without mode-locking. The mode-locking injection increases this power density; however, the improvement in peak amplitude is unknown at this time since it has not been possible to measure the mode-locked pulse widths accurately. The output at 0.53μ was between 10 and 20 milliwatts with a 5 watt average 1.06 micron input at 100 pps. The mode-locking enhancement in the green was approximately a factor of 3.

4.1.1 SHG with Barium Sodium Niobate

At this point in time it was decided to attempt to determine if another SHG material might be usable. The highest theoretically efficient material obtainable at this time is barium sodium niobate which has been shown to damage at power densities of only 1 or 2mW/cm^2 when phase matched and producing SHG. Accordingly, a crystal of this material was placed in the chamber in place of the CD*A. The first crystal chosen was a thin section that had been used on another program and was of extremely poor quality and otherwise unusable. The power density was slowly increased at a low repetition rate and at phase-match temperature to the same level used on the CD*A. No damage occurred and the total green output was on the order of 100 mW. Since no damage occurred it was decided that a high quality barium sodium crystal should be

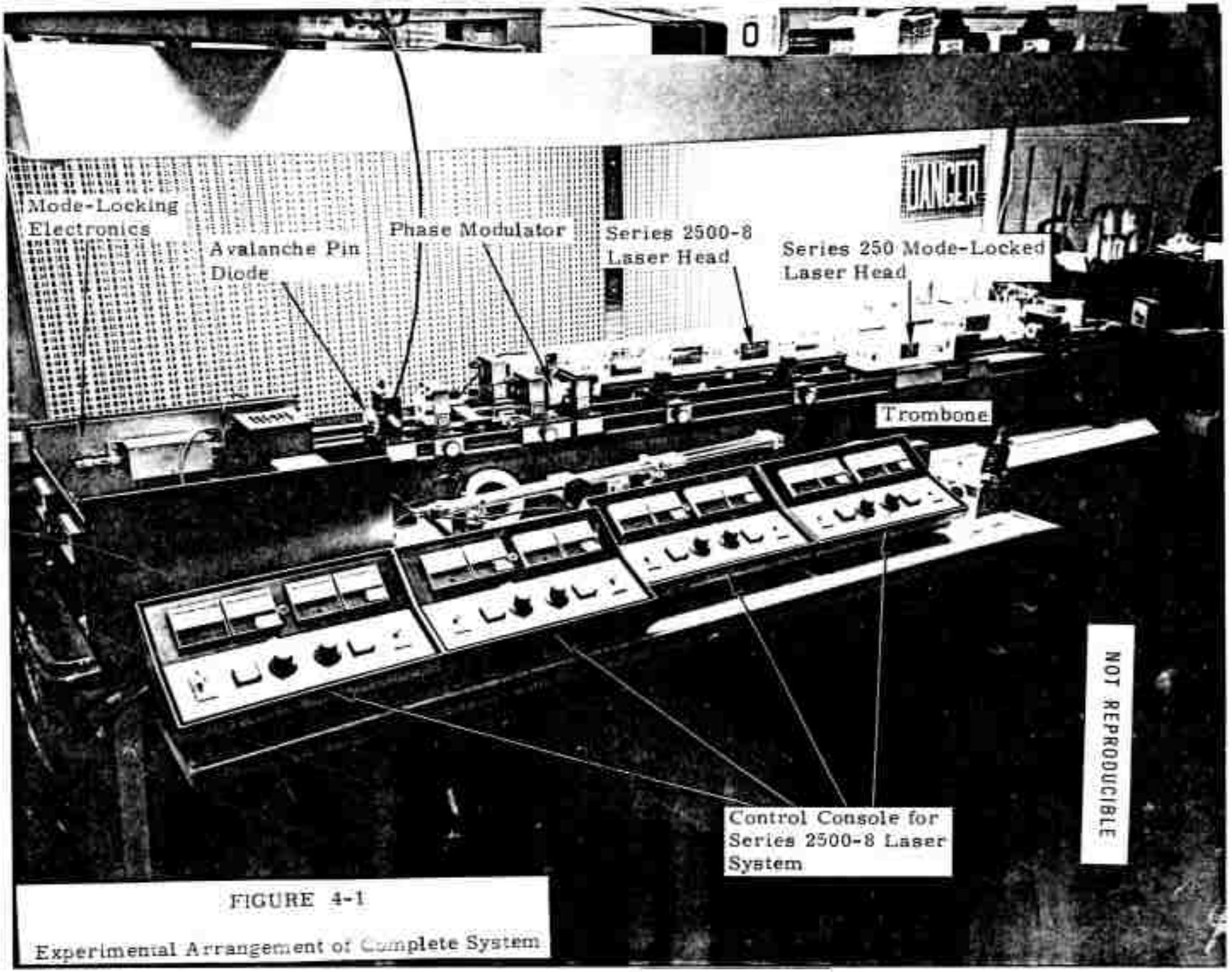

FIGURE 4-1

Experimental Arrangement of Complete System

FIGURE 4-2

Experimental Arrangement of Complete System

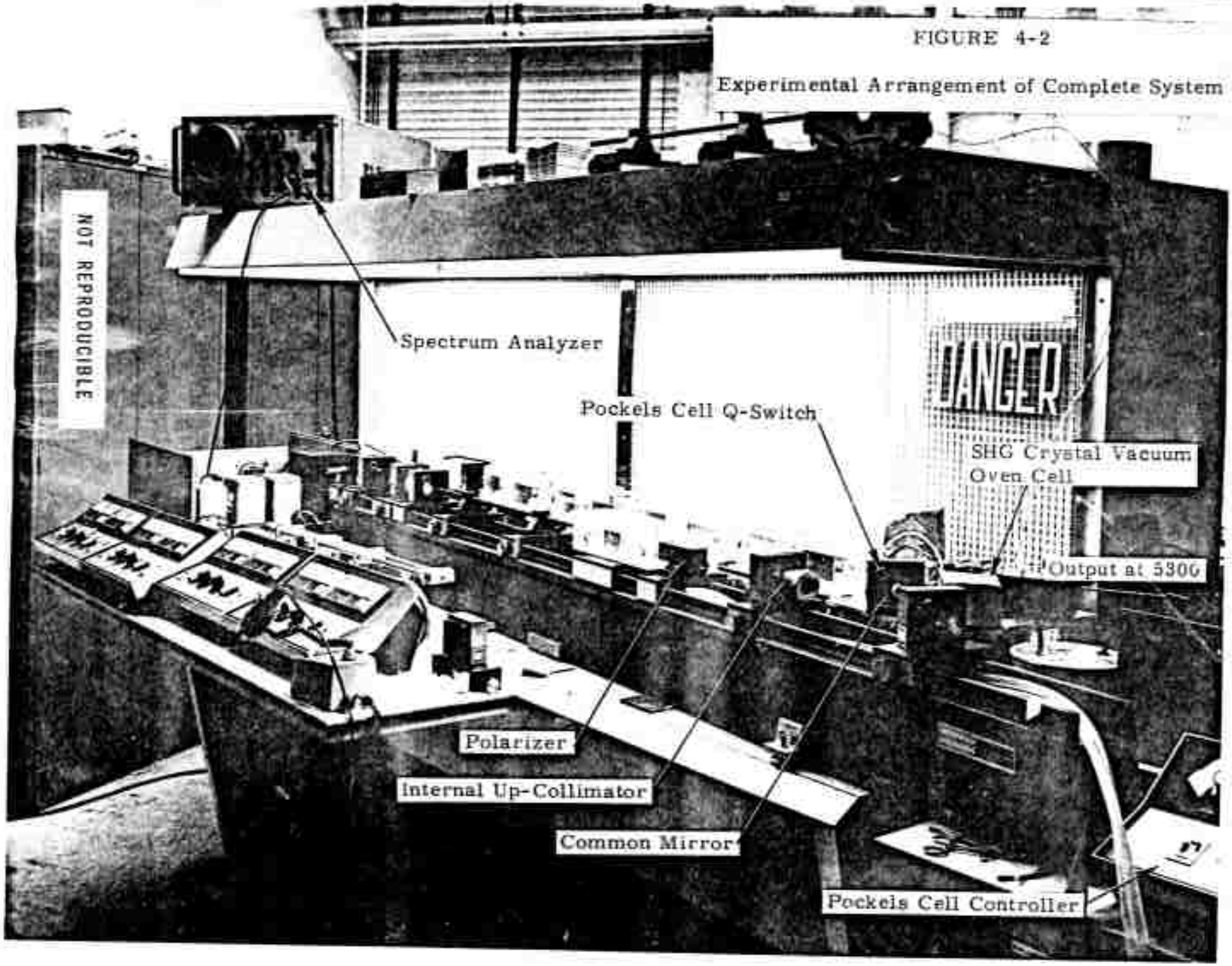

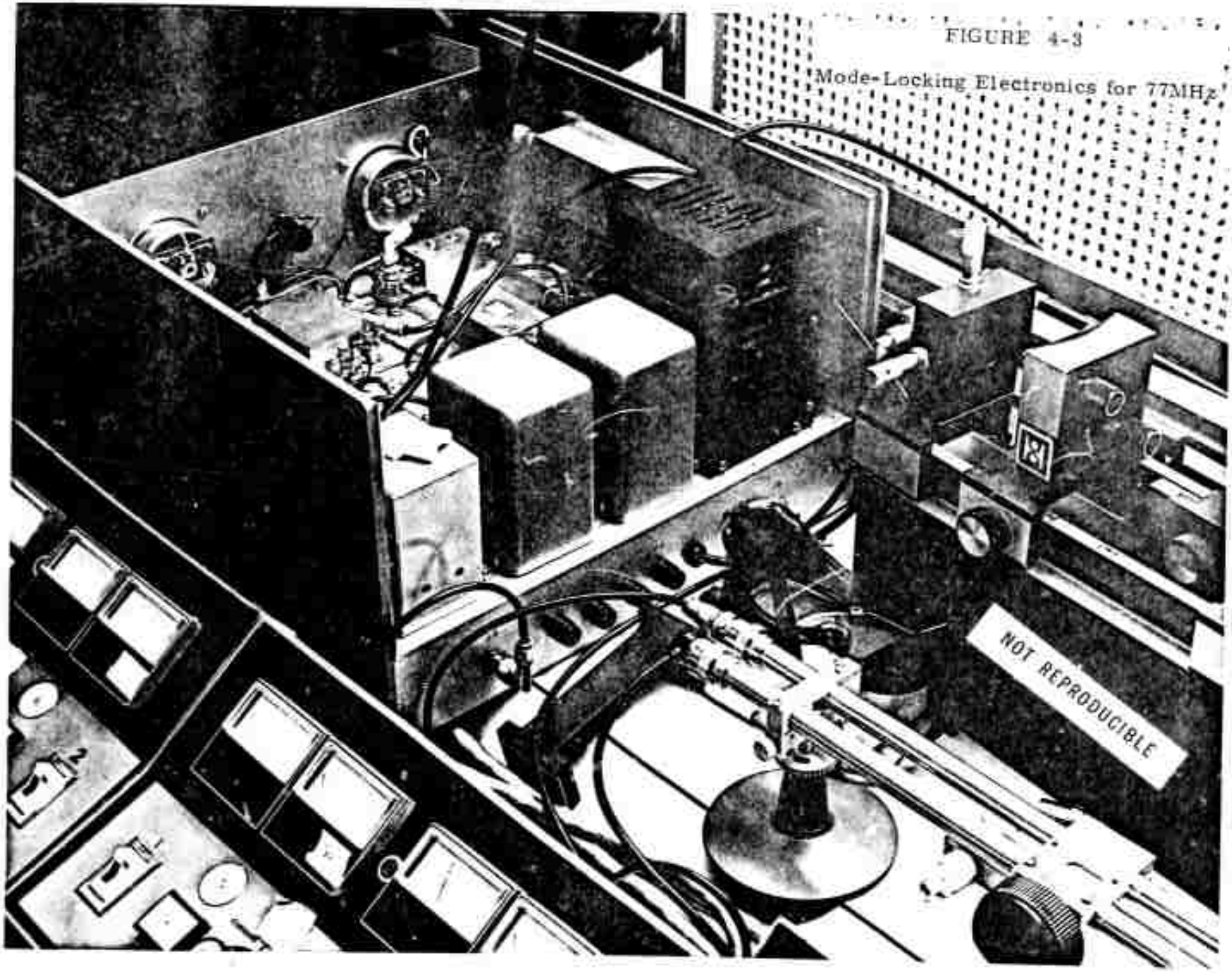

FIGURE 4-3

Mode-Locking Electronics for 77MHz

4-4

FIGURE 4-4

Variable "Trombone" for Phase Control of 77MHz A. F. Signal

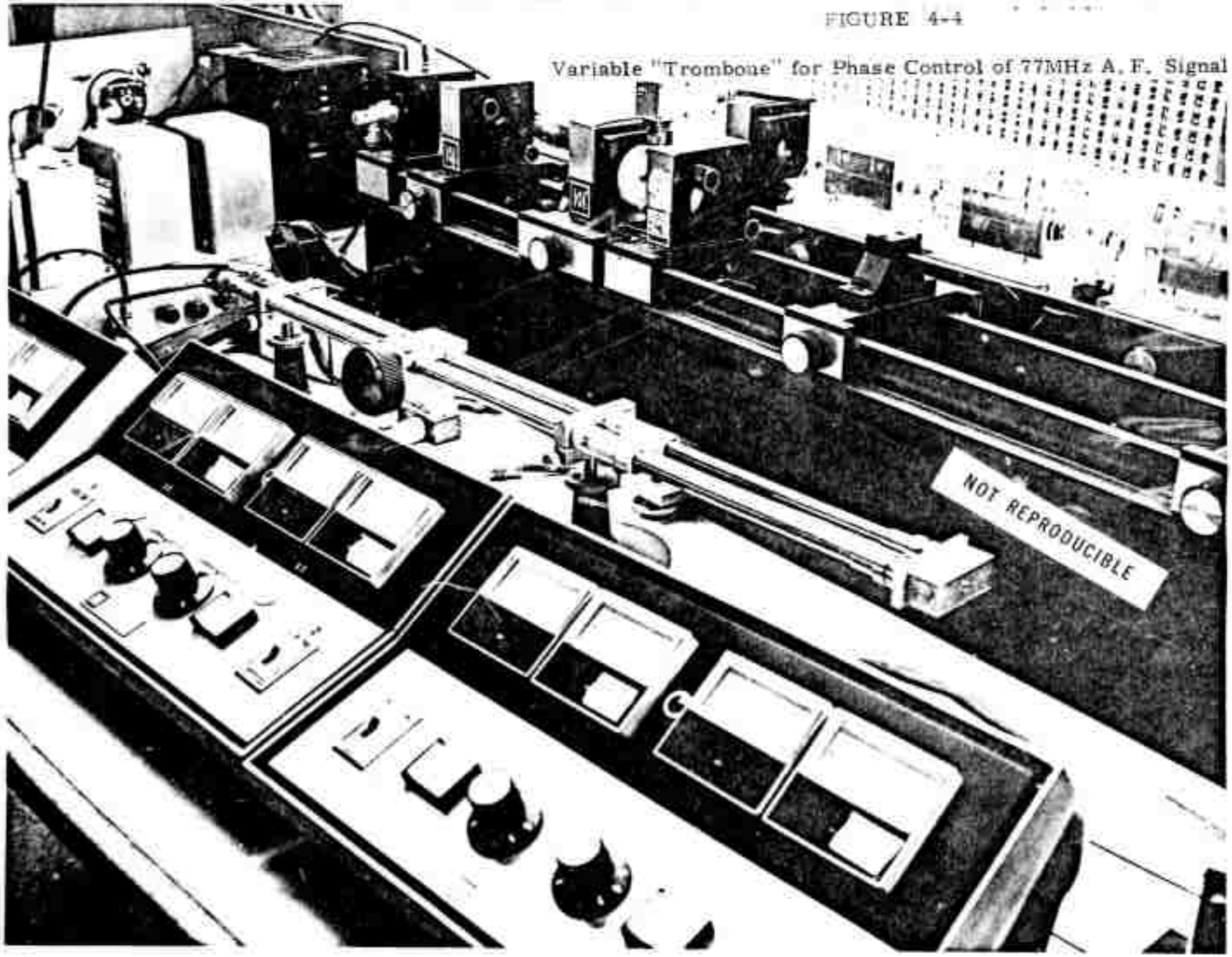

FIGURE 4-5

Series 250 Mode-Locked (Foreground)
Pulse Injection and "C" Switch Pockels
Cell Integration Mechanism (Center-Right)
and Series 2500-8 Laser (Background)

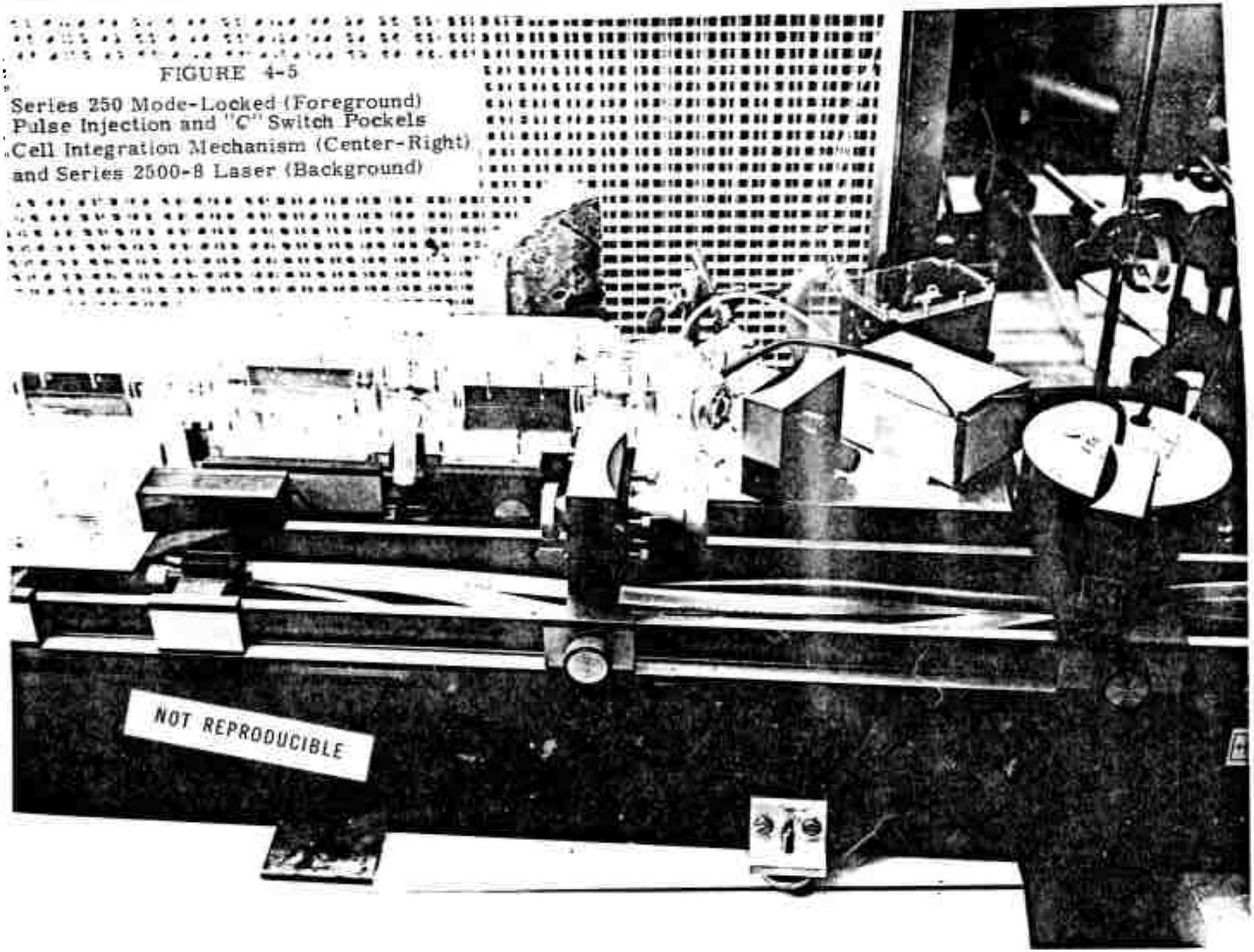

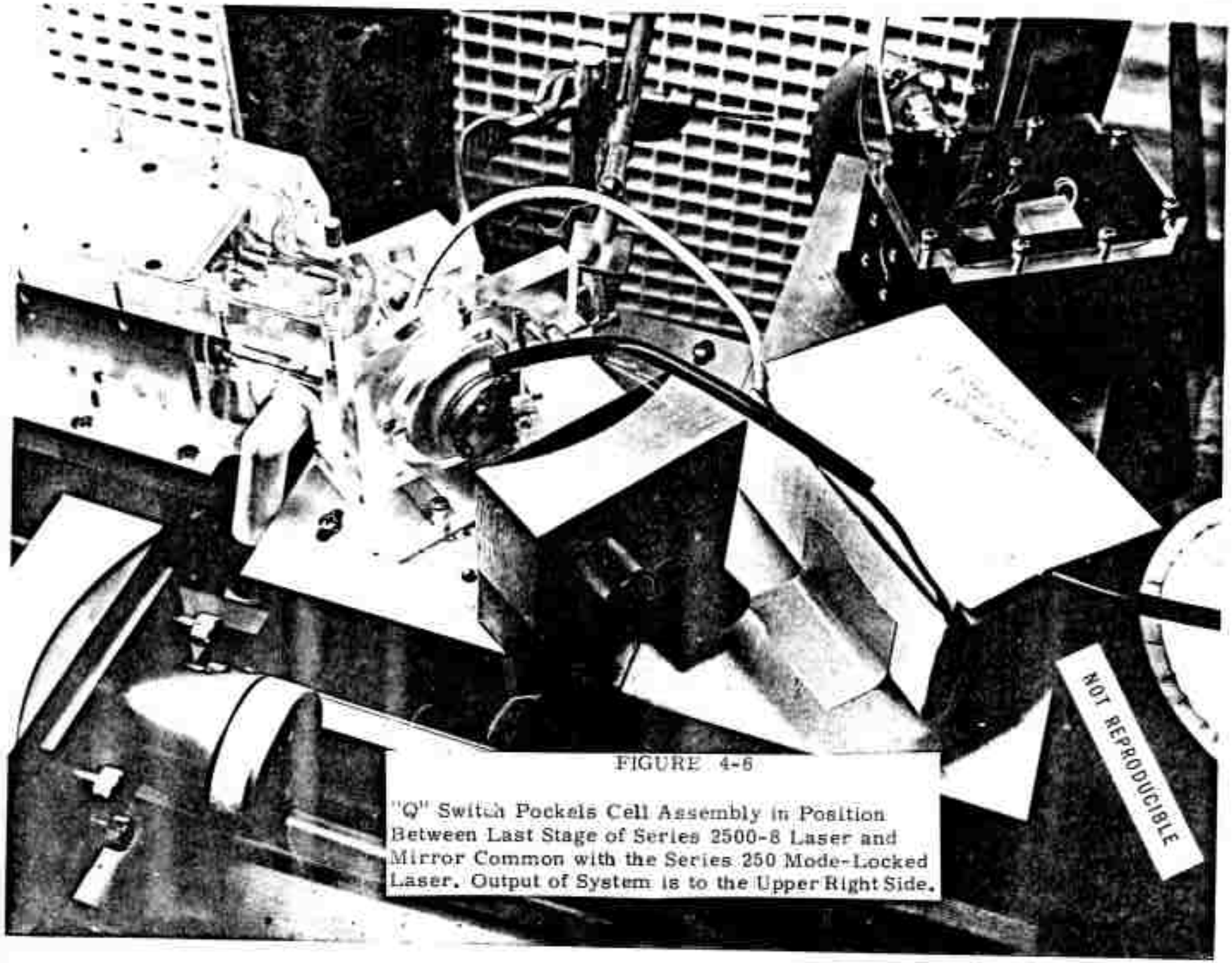

FIGURE 4-6

"Q" Switch Pockels Cell Assembly in Position Between Last Stage of Series 2500-8 Laser and Mirror Common with the Series 250 Mode-Locked Laser. Output of System is to the Upper Right Side.

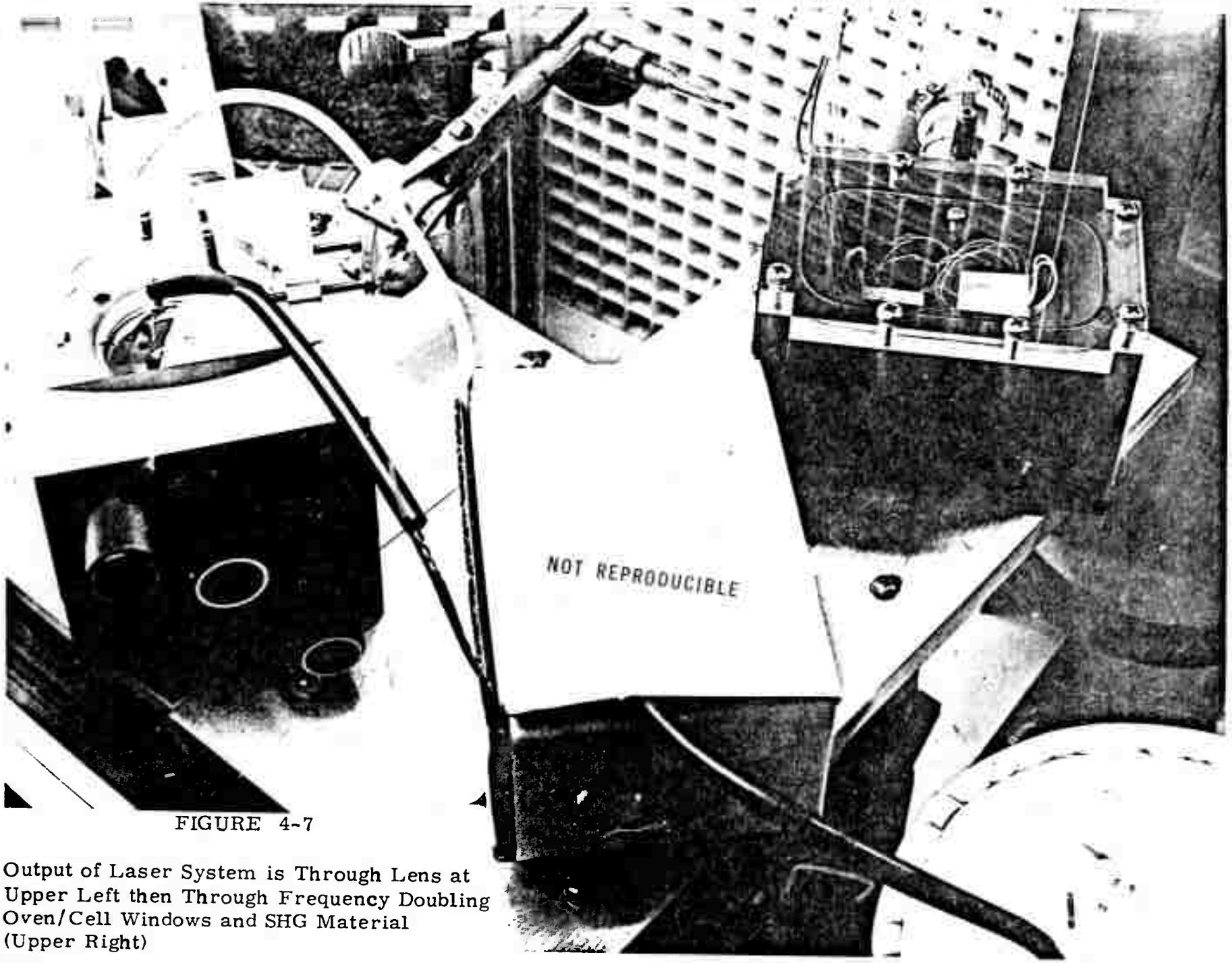

FIGURE 4-7

Output of Laser System is Through Lens at Upper Left then Through Frequency Doubling Oven/Cell Windows and SHG Material (Upper Right)

riskcd. Such a crystal was installcd in the oven. At full powcr in (the beam was apertured to 3/16 inch diameter to fill thc crystal) the total average powcr at 1.06μ passing through the crystal was 6 watts at 100 pps. At phase-match temperature (92°C) the output was 0.7 watts at 0.53μ without mode-locking. When the mode-locked pulses were allowed to dominate the Q-switched pulse the grcen output decreased to approximately 0.3 watts immediately. To check this effect the temperature of the crystal was taken well above the phase-match point (to 125°C) and the mode-locking would indeed enhance the output by a factor of 2 to 3. As the temperature on the crystal was allowed to decrease toward phase match, the mode-locking was turned off and on intermittently showing a decrease in SHG enhancement as phase-match was approached. At an average output (at 100 pps) of 300 mW the mode-locking became ineffective. As the mode-locking was introduced a decrease in 1.06 micron power was noted with no corresponding increase at 0.53μ. (Both the 1.06 micron output and the 0.53μ output were being monitored separately.) As the temperature on the crystal was allowed to decrease further toward phase-match an instantaneous decrease in SHG output would be seen as mode-locking was introduced; then a further decrease would occur as the temperature on the crystal increased further away from phase-match temperature. At the moment the mode-locking was introduced, a corresponding decrease of power would also occur on the 1.06 micron beam passing through the crystal. In other words, power was being lost by some mechanism inside the barium sodium niobate crystal. At phase-match temperature the unmode-locked average output was 0.7 watts and the 1.06 micron average output was 4.5 watts (normal output without SHG was 5.2 watts average). When mode-locking was introduced this output fell to approximately 3.8 watts. Therefore a total power of 0.4 watts (lost at 0.53μ) plus 0.7 watts (lost at 1.06 microns) or 1.1 watts was being lost by some unknown mechanism. It was obvious that this power was being absorbed by the barium sodium niobate crystal since the temperature in the crystal would increase dramatically. To maintain a temperature just above phase-match it was necessary to remove all heating current from the oven. The heating from the absorption process was sufficient to maintain phase-match temperature for 5 to 10 minutes. Eventually, however, the temperature would finally fall just below phase-match and would then fall very rapidly thereafter. If the crystal temperature were increased from below phase-match temperature, as phase-match was approached a thermal runaway would occur taking the crystal temperature

through phase match and then well beyond. This phenomenon has been noted before and is usually referred to as a temperature hangup at phase-match and has been attributed to an absorption at 0.53μ. These tests however, clearly show that it is not associated with absorption at 0.53μ since this would not account for the instantaneous decrease in 5300°A output when mode-locking is introduced. Instead it appears that it may be due to a two-photon process causing an absorption at an equivalent of 0.355μ since barium sodium niobate does have an absorption edge in the near ultra violet. This phenomenon may in fact explain why this material damages at low power densities when phase-matched and the 1.06 micron beam is small in diameter. However, in vivid contrast to earlier experiments in CW second harmonic generation, no surface damage occurred in these tests with a relatively large beam. However an internal damage spot did appear in the form of a series of tiny bubbles, all in a single plane set at approximately 30° to the optical axis. No further tests were performed with barium sodium niobate.

4.1.2 SHG with Lithium Niobate

In an effort to determine if the same effect just described is prevalent in other materials, a crystal of lithium niobate was inserted into the oven in place of the barium sodium niobate. At the same power density and repetition rate as used in the previous test, the lithium niobate produced an output of 0.8 watts average at 0.53μ with mode-locking and 0.3 watts without mode-locking at a phase-match temperature (about 200°C). However by carefully measuring the 1.06 micron output and the 0.53μ output at phase match approximately 0.2 watts of power were missing, presumably absorbed by the lithium niobate by the same or a similar mechanism as in barium sodium niobate. In addition, the same effect of "hanging up" in temperature as the temperature is lowered past phase-match was observed as well as a thermal runaway in approaching the phase-match temperature from below phase match. However the effect was far less severe than in "banana". The power density was subsequently increased in the lithium niobate by lightly focusing the beam. The previous power density was 5 mW/cm^2 and produced an efficiency of approximately 14%. The lens allowed the power density to be increased to 100 mW/cm^2 and the measured output at 0.53μ was 0.6 watts with mode-locking and 0.3 watts without mode locking. Therefore, after increasing the power density by a factor of 20 the efficiency remained constant at approximately 14% indicating a saturated condition. The crystal surface

was very lightly damaged after approximately 60,000 pulses at a power density of 100 mW/cm^2 (not including the mode-locking pulse amplitude enhancement).

4.1.3 SHG with Cesium Dideuterium Arsenate

A one em eube of CD*A was inserted into the oven in place of the lithium niobate and brought up to phase-match temperature slowly (since another crystal had fractured due to cooling too rapidly in another test). At full power input and at 100 pps the average output power at 0.53μ was 0.7 watts mode-locked and 0.35 watts unmode locked. The power density was the same as with lithium niobate at 100 Mw/em^2. During the next series of tests the power density was slowly inereased to 200 MW/cm^2 at whieh point the average output power at 0.53μ had inereased to 1.8 watts mode loeked and 0.6 watts unmode-loeked showing the highest effieieney yet obtained, 25% of the polarized output. The repetition rate was slowly inereased from 100 pps to 200 pps produeing an average output of 2.8 watts at 0.53μ . During subsequent tests the repetition rate was inereased further to 800 pps at which point the average output at 5300°A was a stable 6 watts. By allowing the temperature to drift through the phase-match temperature an output of 7.2 watts was observed at 800 pps. The differenee (see Fig. 4-8) between the effieiency observed at 100 pps (25%) and 800 pps (12%) can be attributed entirely to the temperature differenee aeross the beam within the CD*A erystal eaused by the absorption of 1.06 mierons (See Paragraph 5-2). Only a very slight temperature "hang-up" or thermal runaway was observed at or around the phase-mateh temperature in CD*A indieating far less two photon absorption than in barium sodium niobate or lithium niobate. The table in Fig. 4-9 tabulates the results obtained in all SHG materials tested.

4.1.4 Improved Mode-Loeking Enhaneement

During the course of the previous tests it was observed that when mode-loeking enhancement was employed the primary effeet in SHG enhancement was in the eenter of the beam instead of the eomplete beam as one would expeet. Sinee the Series 250 mode-locked CW YAG laser output beam diameter is on the order of 1mm and the Q-switehed Series 2500 laser utilizes 1/4 ineh diameter rods, it is possible that the beam ratio is preserved and that in fact we are only mode locking the very center of the Q-switched

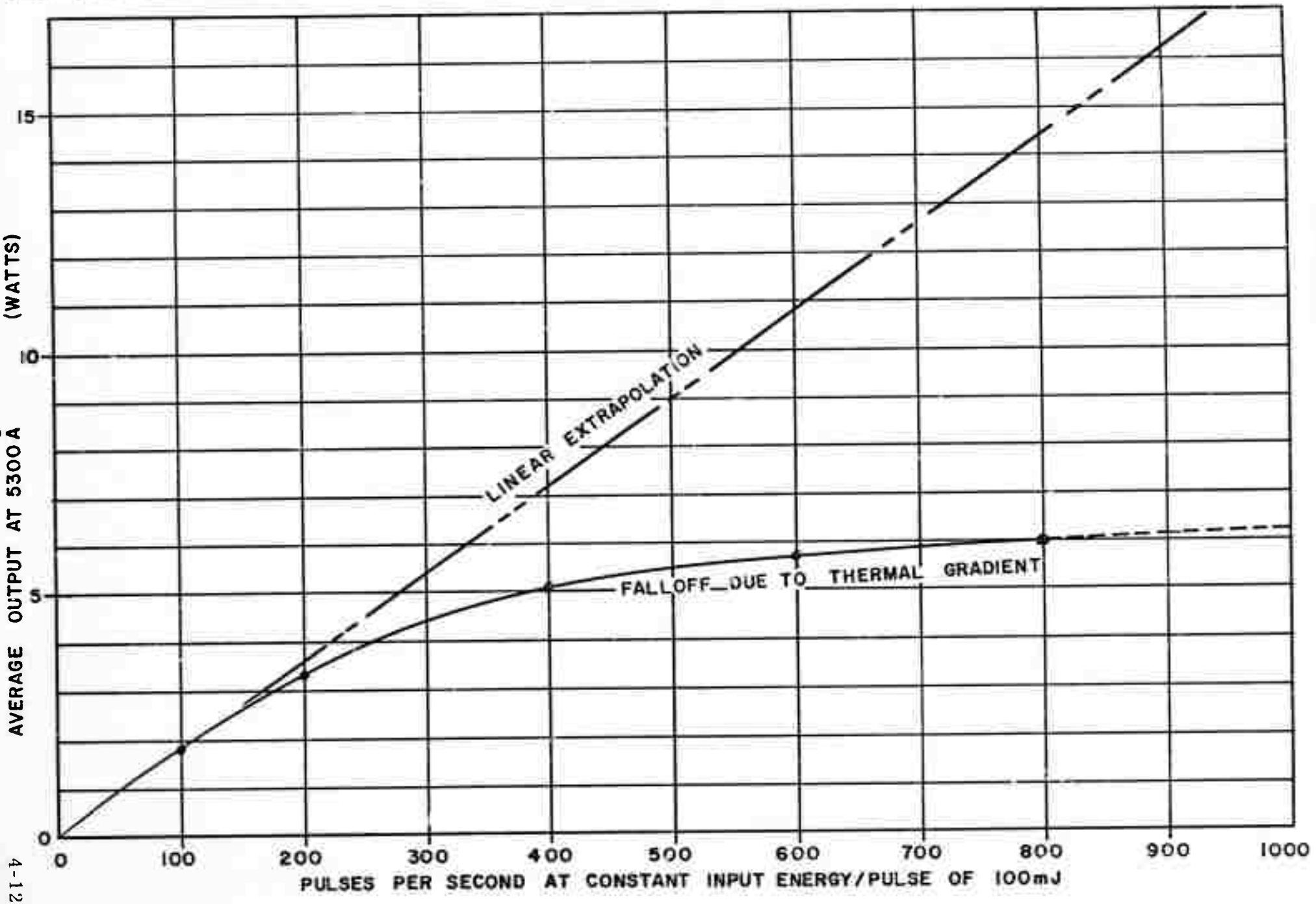
AVERAGE OUTPUT AT 5300 Å (WATTS)
15
10
5
0
LINEAR EXTRAPOLATION
FALLOFF DUE TO THERMAL GRADIENT
0
100
200
300
400
500
600
700
800
900
1000
PULSES PER SECOND AT CONSTANT INPUT ENERGY/PULSE OF 100mJ

FIGURE 4-8

LENGTH	MATERIAL	POWER DENSITY IN MW/cm^2						
		5	M.L. ▲	100	M.L. ▲	200	M.L. ▲	M.L. ▲▲
5 mm	$BaNaNb_5O_{15}$	12%	6%					
5mm	$LiNbO_3$	7%	14%	7%	12%			
1cm	CsD_2AsO_4	.1%	1%	4%	12%	10%	25%	40% ▲▲▲
2 cm	KD_2PO_4		.1%			.5%	1.5%	2.5%

▲ LOW EFFICIENCY MODE LOCKED

▲▲ HIGH EFFICIENCY MODE LOCKED

▲▲▲ EXPECTED EFFICIENCY BASED ON RESULTS OF KD_2PO_4

FIGURE 4-9

TABLE OF MEASURED SINGLE PASS EFFICIENCY OF SHG MATERIALS

output beam. In an effort to determine whether this is occurring a 5:1 up collimator was installed inside the cavity of the CW mode-locked system increasing the injected beam diameter to 5mm. In attempting to evaluate the effect of this larger beam, the CD*A crystal was destroyed, not because of the mode-locking enhancement but because a high rep rate high average power beam was introduced into the crystal too rapidly causing a thermal strain and fracturing the crystal. Since another CD*A crystal was not immediately available, a KD*P crystal (2 cm in length) was installed and the enhancement was checked. Where previously a SHG enhancement ratio of 3 to 1 was typical, the new enhancement ratio is 5 to 1. The KD*P produced an average 0.53μ output of 0.3 watts mode-locked at 100 pps and 0.060 watts non-mode-locked. Increasing the repetition rate to 600 pps produced a linear extrapolation to 1.8 watts average power output at 0.53μ .

4.1.5 SHG Experiment Conclusions

The data presented in this section clearly indicates that cesium dideuterium arsenate is the only SHG material studied which has any reasonable probability of reaching the basic goals of this development program. At low repetition rates it is reasonable to expect overall efficiences in excess of 50% by utilizing the 5 to 1 enhancement technique and a 2 cm long crystal at a power density (unmode-locked) of 200 Mw/cm^2. At high repetition rates the absorption at 1.06 microns will still present a problem in terms of the thermal loading on the crystals and the temperature gradient across the beam.

SECTION V

SOME THEORETICAL CONSIDERATIONS

We have not attempted in this first report to present a complete theoretical analysis of the laser system or the harmonic conversion process. There are, however, several special points which should be covered.

5.1 Possible Source of Crystal Heating

The linear absorption of our $Ba_2NaNb_5O_{15}$ crystals at 1.06μ and in the vicinity of 0.53μ (.5145μ from argon ion laser) has been measured, and the results indicate that these coefficients are both much too small to produce the observed crystal heating. Therefore, some non-linear absorption process must be responsible. Phase-matched third harmonic generation followed by absorption of the third harmonic is not possible because of the high linear absorption at the third harmonic. Phase-matched interactions will grow only if the interacting fields can propagate; a strong absorption for any one of the fields limits the interaction length such that the energy converted by the parametric process is negligible. Thus, the strong absorption at the third harmonic frequency itself prevents the phase-matched process.

When the absorption at the higher harmonic is large, however, a two photon absorption process (e.g., one SH photon plus one fundamental photon) is possible. In this case, phase-matching is not important because there is no traveling wave interaction; the photon energy is absorbed throughout the material (as in linear absorption).

To get an idea of the effect of this type of absorption on the SHG process, we will introduce it into the traveling wave equations for SHG. Since the magnitude of the effect we observe is of the order of the SHG process, we can use the same approximations in the wave equation as those that are used to analyze parametric interactions. Neglecting linear loss, the wave equation becomes:

$$ik_n \frac{dE_n}{dZ} \; e^{i(\omega_n t - k_n Z)} + C.C. = -\mu_o \frac{\partial^2}{\partial t^2} \left[P_n^{N.L.} (Z_1 t) \right] \quad (1)$$

where the subscript n refers to a particular Fourier component of the electric or polarization field. The term $P^{N.L.}$ includes only nonlinear terms in the electric field, the linear term having been included in the L.H.S. Thus,

$$P_n^{N.L.} = P_n - XE_n = dE_n^2 + \epsilon E_n^3 + \ldots \quad (2)$$

The pertinent term in this expansion for two-photon absorption can be obtained from the term in Poyntings Theorem for the power expended in polarizing the dielectric:

$$\text{Power lost} = \overline{E \frac{\partial P}{\partial t}} \quad (3)$$

Substituting from eq. 2,

$$\text{Power lost} = \sum_n i\omega_n \left(X E_n^2 + d E_n^3 + \epsilon E_n^4 + \ldots \right) \quad (4)$$

Thus, two photon absorption implies a negative imaginary coefficient for the fourth power term in the electric field. Therefore

$$\epsilon = -i\epsilon' \quad (5)$$

where ϵ' is real.

Assuming an electric field of the form

$$E(Z_1 t) = E_1(Z) e^{i(\omega_1 t - k_1 Z)} + E_2(Z) e^{i(\omega_2 + -k_2 Z)} + C.C.$$

where the subscripts 1 and 2 refer to the fundamental and SH fields, respectively, and substituting into eqs. (2) and (1), we get

$$\frac{d E_2(Z)}{dZ} e^{i(\omega_2 t - k_2 Z)} = \frac{-\mu_o}{i k_2} \frac{\partial^2}{\partial t^2} \left[\frac{d}{4} E_1^2 e^{i(2\omega_1 t - 2k_1 Z)} - i \frac{3}{4} \epsilon' E_1 E_1^* E_2 e^{i(\omega_2 t - k_2 Z)} \right]$$

Assuming perfect phase-matching for the SHG process, i.e., $k_2 = 2k_1$ this becomes

$$\frac{dE_2}{dZ} = -i K E_1^2 - \alpha \left| E_1 \right|^2 E_2 \tag{6}$$

where

$$K \triangleq \frac{\omega_2 \mu_o d}{4 k_2}$$
$$\alpha \triangleq \frac{3\omega_2^2 \mu_o \epsilon'}{4 k_2} \tag{7}$$

To simplify the analysis, we will neglect pump depletion; i.e., assume E_1 = const. This is a good assumption in our case because the observed conversion efficiencies were always less than about 15%.

Note that the field amplitudes are, in general, complex quantities and a solution with a phase variation in Z is conceivable. However, if a solution with no phase variation is possible, it will dominate because the gain mechanism will not be divided to drive both amplitude and phase. Therefore, we will look for a solution with stationary phase. Rewriting E_1 as

$$E_1 = E_{10} e^{i\varphi_1} = \text{Constant}$$

and still allowing $E_2(Z)$ to be complex, eq. (6) becomes

$$\frac{dE_2}{dZ} = K E_{10}^2 e^{i(2\varphi_1 - \pi/2)} - \alpha E_{10}^2 E_2$$

This can be easily solved for E_2:

$$\left\{ \frac{dE_2}{KE_{10}^2 \left[e^{i(2\varphi_1 - \pi/2)} - \frac{\alpha}{K} E_2 \right]} \right\} = dZ$$

$$\left(-\frac{K}{\alpha} \right) \frac{1}{KE_{10}^2} \ln \left[e^{i(2\varphi_1 - \pi/2)} - \frac{\alpha}{K} E_2 \right] = Z + C$$

$$e^{i(2\varphi_1 - \pi/2)} - \frac{\alpha}{K} E_2 = C e^{-\alpha E_{10}^2 Z}$$

@ $Z = 0$, $E_2 = 0$, therefore $C = e^{i(2\varphi_1 - \pi/2)}$

and,

$$E_2(Z) = \frac{K}{\alpha} \left[1 - e^{-\alpha E_{10}^2 Z} \right] e^{i(2\varphi_1 - \pi/2)}$$

Thus, a stationary phase solution does exist with $\varphi_2 = 2\varphi_1 - \pi/2$. This is the usual phase relationship for maximum SHG.

This relationship is plotted below for three different crystal lengths, Z = L

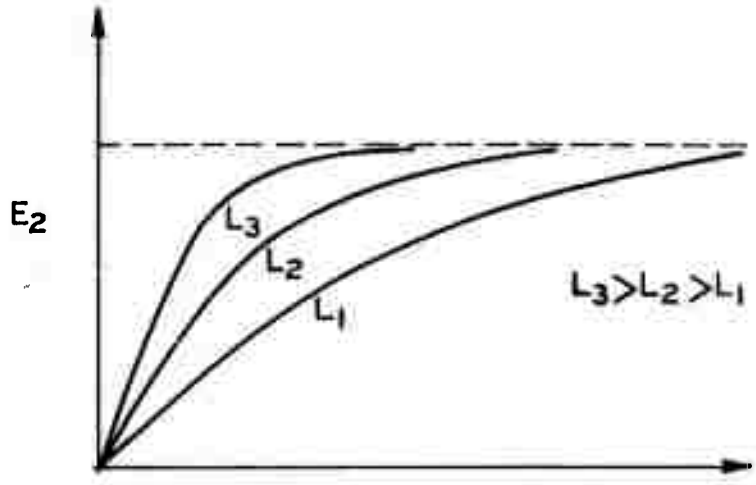

$$E_{10}^2 \propto \frac{P_1}{A}$$

Note that this predicts a saturation in the SH output which is independent of pump power density and crystal length.

This is in fact quite similar to the saturation observed experimentally, except that in some cases, the SH amplitude was seen to go through a maximum and decreased with increasing pump power. This may indicate that additional nonlinear absorption processes were in effect. Other possible loss mechanisms are absorption by photoinduced carriers or by excited-state absorption.

In two instances reported in the literature[2], [3] authors have concluded that these latter mechanisms were primarily responsible for observed nonlinear absorption. Both experimental situations were similar to the one described here. (In the case of reference 3, the absorption caused a limitation of SHG efficiency from 1.06μ to 5.3μ in Tellerium.) In both cases a two-photon absorption process produced the carriers or excited states which then acted as absorption centers for the fundamental field. Also, in both cases, the absorption due to these induced carriers or excited states was shown to be much larger than that due to the two-photon process alone.

5.2 Phase-Match Degradation Due to Absorption

Absorption of laser radiation in the SHG crystal creates a temperature profile across the beam region, making it impossible to maintain perfect 90° phase-matching over the entire beam cross section. We have seen this effect using clearly both in low power CW SHG with $Ba_2NaNb_5O_{15}$ and high power SHG with CsD_2AsO_4. A calculation of the expected degradation in second harmonic conversion efficiency as the laser average power is increased is presented here.

Our experiments were conducted with a square crystal with a heat sink on only one side. We simplify this geometry for computation purposes to be an infinite cylindrical crystal with heat sink on the entire surface, with the beam centered on the cylinder axis. We also assume constant power density in the beam. In this case we have a temperature profile over the beam.

$$T(r) = \underbrace{T_o + \overbrace{\frac{P\beta}{4\pi k}}^{\Delta T_c}\left[1 + 2\ell n \frac{R}{w_o}\right]}_{T_A} - \frac{r^2}{w_o^2}\Bigg]$$

$$= T_A - \Delta T_c \frac{r^2}{w_o^2}$$

where
- r = distance from crystal beam center
- ΔT_c = temperature differential across beam
- P = Laser power (watts)
- β = absorption coefficient (cm^{-1})
- k = termal conductivity (watts $^oC^{-1}$ cm^{-1})

The relative SHG conversion efficiency as a function of temperature is G (T), nominally a $\sin^2 x/x^2$ form.

$$P\,(2\omega) = \text{green power} \;\alpha\; \int_0^{\omega_o} 2\pi r\, G\,\left[T\,(r)\right]\, dr$$

For arithmetic ease we assume that

$$G\,(T) = e^{-\gamma\, 2(T-T_M)^2}$$

where T_M = phase-match temperature

$$P\,(2\omega) \;\alpha\; \int_0^{\omega_o} r\, e^{-\gamma^2 \left(T_A - T_M - \Delta T_c \frac{r^2}{\omega_o^2}\right)^2} dr$$

Assume $T_A = T_M$, implying exact phase-match at the crystal center.

yielding

$$\frac{P\,(2\omega)}{P_o\,(2\omega)} = \left(\frac{\pi}{8\,\ell n 2}\right)^{\frac{1}{2}} \left(\frac{\Delta T_M}{\Delta T_c}\right) \text{ erf } \left(2\,\ell n^{\frac{1}{2}} 2\;\frac{\Delta T_c}{\Delta T_M}\right)$$

where $\Delta T_M = \dfrac{2\,\ell n^{\frac{1}{2}} 2}{\gamma}$ = full width at $\frac{1}{2}$ maximum

$P_o(2\omega)$ = low rep rate (no thermal effect) green power

since $\Delta T_c = \dfrac{P(\omega)\,\beta,}{2\pi\, k}$

if we define η as the low rep rate efficiency

$$P\,(2\omega) = \eta\left(\frac{\pi^3}{2\ell n 2}\right)^{\frac{1}{2}} \quad \frac{\Delta T_M\; k}{\beta} \quad \text{erf}\left(\frac{\ell n^{\frac{1}{2}}\, 2}{\pi\, k} \quad \frac{P\,(\omega)\,\beta}{\Delta T_M}\right)$$

Since $\text{erf}\,(x) \underset{x\to\alpha}{\longrightarrow} 1$, the average second harmonic power saturates at a level

$$P\,(2\omega)_{\max} = \eta\left(\frac{\pi^3}{2\ell n 2}\right)^{\frac{1}{2}} \quad \frac{\Delta T_M\; k}{\beta}$$

e.g. $\eta = 0.25$

$\Delta T_M = 5.6^{o}C$

$k = 0.018$ (estimated for CD*A) watts $^{o}c^{-1}$ cm^{-1}

$\beta = 0.009\ cm^{-1}$

$$P_{max}(2\omega) = 0.25\ (4.7)\ (5.6)\ \frac{(1.8) \times 10^{-2}}{0.9 \times 10^{-2}}$$

$$P_{max}(2\omega) = 13.2 \text{ watts}$$

The observed saturation level was approximately 8 watts. The 30% disagreement can be explained qualitatively by the fact that the crystal had a heat sink on only one side, causing a larger normal gradient. Further, the exact mathematical form of the phase-match curve should be used in the calculations. The results would also be modified if we took into account saturation in the conversion process.

We conclude from this brief exercise that theoretically we can expect to observe a saturation in the average second harmonic power, the saturation level depending linearly on the phase-match temperature half width and the thermal conductivity and inversely on the absorption coefficient. Our experimental results confirm the calculations, at least approximately, and give support to our understanding of the limitations on harmonic conversion efficiency at high average powers.

5.3 Pulse Width Degradation

A short pulse transmitted through an amplifier with finite bandwidth will suffer an increase in pulse-width. In order to determine the limitations of the mode-locked pulse injection technique we will calculate the theoretical pulse broadening which occurs in the four-five transits through the high gain CW regenerative amplifier.

We assume a Gaussian pulse having an amplitude

$$f_1 = \exp\left[-\alpha t^2\right]$$

propagated through an amplifier medium with complex gain

$$G(\omega) = \exp\left\{ g_o \left[1 - jT_2(\omega-\omega_o) - T_2^{\,2}(\omega-\omega_o)^2\right]\right\}$$

yielding a new pulse, obtained by Fourier transformation

$$f_2 = \int G(\omega)\, g(\omega)\, e^{j\omega t}\, d\omega$$

where

$$g(\omega) = \frac{1}{2\pi}\int \exp\left[-\alpha t^2 + j(\omega_o - \omega)t\right] dt$$

$$= \frac{1}{2\pi^{\frac{1}{2}}}\ \frac{1}{\alpha^{\frac{1}{2}}}\ \exp\left[-\frac{(\omega-\omega_o)^2}{4\alpha}\right]$$

yielding

$$f_2 = \frac{e^{g_o}\, e^{j\omega_o t}}{(1 + 4\alpha\alpha_o L T_2^{\,2})^{\frac{1}{2}}}\ \exp\left[\frac{-\alpha(t - g_o T_2)^2}{1 + 4\alpha g_o T_2^{\,2}}\right]$$

Ignoring the phase term, we see that the new pulse has a new Gaussian shape parameter

$$\alpha + \Delta\alpha = \frac{\alpha}{1 + 4\alpha g_o T_2^{\,2}}$$

Since $\frac{2^{\frac{1}{2}}}{\pi}\ \frac{1}{T_2} = \Delta f_{at}$ = atomic line width

and $\tau_{\frac{1}{2}} = 2^{\frac{1}{2}}\ \ell n\ 2\alpha^{-\frac{1}{2}}$ = pulse-width

$$\frac{\Delta\tau_{\frac{1}{2}}}{\tau_{\frac{1}{2}}} = \frac{2\ell n^2 2}{\pi^2}\ \frac{g_o}{(\Delta f_{at}\cdot\tau_{\frac{1}{2}})^2}$$

For one pass of a 0.2 nanosecond pulse through the amplifier (round trip).

$$g_o = 6$$

$$\Delta f_{at} = 1.6 \times 10^{11} \text{ Hz}$$

$$\tau_{\frac{1}{2}} = 2 \times 10^{-10}$$

$$\frac{\Delta \tau_{\frac{1}{2}}}{\tau_{\frac{1}{2}}} = 0.00058$$

In 5 transits the maximum fractional increase in pulse-width is

$$\left(\frac{\Delta \tau_{\frac{1}{2}}}{\tau_{\frac{1}{2}}} \right)_5 = 0.003$$

The effect would be larger for shorter pulses, but we do not anticipate achieving a pulse width shorter than about 0.12 nanoseconds in the long 77MHz cavity. Therefore pulse broadening due to the amplifier bandpass can be neglected.

REFERENCES

(1) A. Yariv, Quantum Electronics, John Wiley & Sons, Inc., 1967, p 350, Eq. 21.4-10.

(2) A. Hordvik, "Pulse Stretching Utilizing Two Photon Induced Light Absorption", pre-print from Air Force Cambridge Research Labs.

(3) W. B. Gandrud & R. L. Abrams, "Reduction in SHG Efficiency in Tellurium by Photoinduced Carriers," Ap. Phy. Lett. 17, 7, 302, (1970).

SECTION VI

CONCLUSIONS

From the results of the program thus far we can conclude:

1. Mode-locked pulse injection combined with Q-switching in a CW high power Nd:YAG laser can be made to function reproducibly, creating substantial increases in laser peak power, which in turn yields a substantial enhancement in second harmonic conversion efficiency.

2. We have demonstrated that by using cesium dideuterium arsenate we can obtain harmonic conversion efficiencies of 25% to 40% with a multitransverse mode laser through the use of 90° phase matching.

3. We have demonstrated a saturation in second harmonic average power resulting from a temperature gradient across the beam due to 1.06μ absorption.

4. We have discovered what is apparently a fundamental limitation in the use of barium sodium niobate and lithium niobate in the form of a severe thermal heating at conversion efficiencies exceeding a few percent. Evidence points to two photon absorption as the source of this heating.

5. We have produced 7.2 watts at 0.53 microns, approximately a factor of two less than we would have achieved were it not for the thermal gradient effects in the cesium dideuterium arsenate crystal. We have obtained this at a laser pulse repetition frequency of 800 pps, approximately a factor of five slower than the rate at which the laser can be expected to operate with only a slight degradation in pulse peak power.

6. The cesium dideuterium arsenate crystals have been able to withstand the peak powers required to yield high conversion efficiencies of greater than 50%.

The general conclusion that we have reached is that in order to produce average powers at 0.53 microns of greater than 20 watts it will be necessary to take steps to alleviate the thermal limitations of the harmonic generating crystals. This can be accomplished through an improvement in the materials themselves and the use of mechanical techniques which either distribute the thermal loading over a larger crystal volume or improve markedly the rate of heat removal. A discussion of these techniques will be presented in the final report.

It should be possible to obtain an improvement in second harmonic power by approximately a factor of 2.5 by improving the mode-locked pulse injection technique and the polarization characteristics of the laser.

SECTION VII

PLANS FOR THE REMAINDER OF THE PROGRAM

In an effort to circumvent the thermal loading problem, a flowing fluid cell will be designed to hold two CD*A crystals in series which have previously been matched for identical phase-match temperature. The fluid temperature will be controlled and thereby allow the crystals to be held at phase-match temperature on all six sides of each crystal. This technique should allow a higher repetition rate to be achieved at a higher overall efficiency since the heat removal should be at least twice as fast as in the present oven. In addition, work is continuing on a higher repetition rate Pockels cell voltage pulser which should allow the system to reach at least 1600 pps.

The combination should yield a substantial increase in average power at 0.53u. We hope to produce a minimum of 20 watts as compared with our previous maximum of 7.2 watts.

SECTION VIII

SUGGESTIONS FOR CsD_2AsO_4 CRYSTAL IMPROVEMENT

The single item which would benefit this program the most but is beyond its scope would be a reduction in the absorption coefficient of CD*A at 1.06 microns by an order of magnitude.

A comparison of the optical transmission curves for deuterated CsD_2AsO_4 and KD_2PO_4, Figure 3-3 shows a substantially reduced cutoff for CsD_2AsO_4 at both the ultraviolet and infrared ends of the visible spectrum. The fact that ultraviolet transmission for a 1.0 centimeter length of CsD_2AsO_4 is reduced to 50% at 0.24 microns may be an inerent feature of the arsenates versus the phosphates. However, the pronounced dip near 0.35 microns may be due to impurity contamination. At the infrared end greater than twice the absorption at 1.50 microns in CsD_2AsO_4 versus KD_2PO_4 suggest that hydrogen contamination may be present; i.e., the CsD_2AsO_4 sample measured was not as fully deuterated as the KD_2PO_4 sample measured. In fact, it is quite probable that neither sample was fully deuterated. Careful control of the growth parameters for both the tetragonal phosphates and arsenates is therefore imperative if repeatable results are to be ensured.

Since CsD_2AsO_4 has been demonstrated to be a highly important material for 90 degree phase-matched optical frequency doubling of 1.065 micron laser output, it is essential that everything possible be done to improve its optical properties. Dominating these properties presently is the absorption at both 1.054 and 0.533 microns, which must be reduced beyond the current state-of-the-art. Also there are indications that sum-frequency generation may also pose an ultimate thermal limitation upon the material. Since this sum frequency corresponds to a wavelength of 0.355 microns, at the dip in the transmission curve referred to above, it is important to know whether indeed contamination due to growth additives or other chemical impurity is responsible.

A review of several factors influencing CsD_2AsO_4 single crystal growth is presented below. The ultimate aim of a program to improve CsD_2Aso_4 from the standpoint of its optical properties would be to refine each of the growth parameters to a logical and scientifically understood set of operating conditions, thereby removing many of the uncertainties which have kept crystal growing in the realm of a mysterious art.

First, the elimination of all chemical impurities from the starting materials is of utmost importance. Since CsD_2AsO_4 is grown from an acid solution prepared from an admixture of $CsAsO_3$ in $DAsO_3$, there are very few initial ingredients to be checked for purity. Careful control of the cesium salts should be possible by ordinary chemical preparation techniques. Deuterated arsenic acid, derived from the reaction:

$As_2O_5 + D_2O \longrightarrow 2\ (DAsO_3)$ should be prepared in a dry Argon atmosphere to avoid any possibility of water vapor infiltration. The D_2O itself should be obtainable to better than 99.7% purity from certified government sources.

Second, the growth rate and starting temperature must be judiciously chosen to coincide with the degree of supersaturation both initially and at the end of the growth run. Problems due to tapering of the crystal boules and the inability to sustain a uniform growth rate will adversely affect the optical quality of the finished crystals. Although some experimenters have attempted to introduce trace impurities in order to counter such adverse effects, it is felt that a wiser choice would be to add nothing additional to the growth solution. Rather, a careful search should be made for a temperature regime over which a run could be successfully made without requiring additives. The growth rate achievable under the conditions established above will be determined primarily by the starting temperature and pH factor under optimum supersaturation conditions. Hopefully it will be fast enough to attain an economic yield within three to four months time. Faster growth rates should be avoided since optical homogeneity will suffer if the growing speed is excessive.

Third, thermal gradients and uneven stirring should be avoided since striae and optical index gradations will result. Furthermore, the rotational speed of the crystals, if they are grown in a modified Holden apparatus, should not exceed that required to produce uniform growth along the principal Z-axis direction. While some agitation is necessary, excess or uneven turbulence should be avoided. The physical placement of the growth chamber should be in a room, preferable in a sub-basement location, which will be subject to as little vibration and temperature fluctuation as possible. Adequate fiber glass insulation and remote electronic temperature control would appear preferable.

Fourth, consideration should be given to the preparation of "seed" material in the form of carefully prepared 0-degree Z-axis platelets. It is imperative that all residual material be carefully removed from the seed faces to guarantee uniform "capping-over" as the growth is started. Great care must be given to the rate of insertion and temperature of the seeds as they are being lowered into the growing nutrient bath.

Lastly, thorough attention to detail, both in preparation of the nutrient solution and initiation of a growth run will require great patience on the part of the crystal grower. The remainder of the run, lasting for several months, must be fully automated and should include the use of reliable methods of temperature control and an emergency power source to avoid loss of the runs in the event of a local power failure.

HOLOBEAM'S Nd:YAG Mode-Locking System. . .

STAYS

LOCKED

using the

CLOSED-LOOP

PHASE-MODULATION

technique

described

in this

article

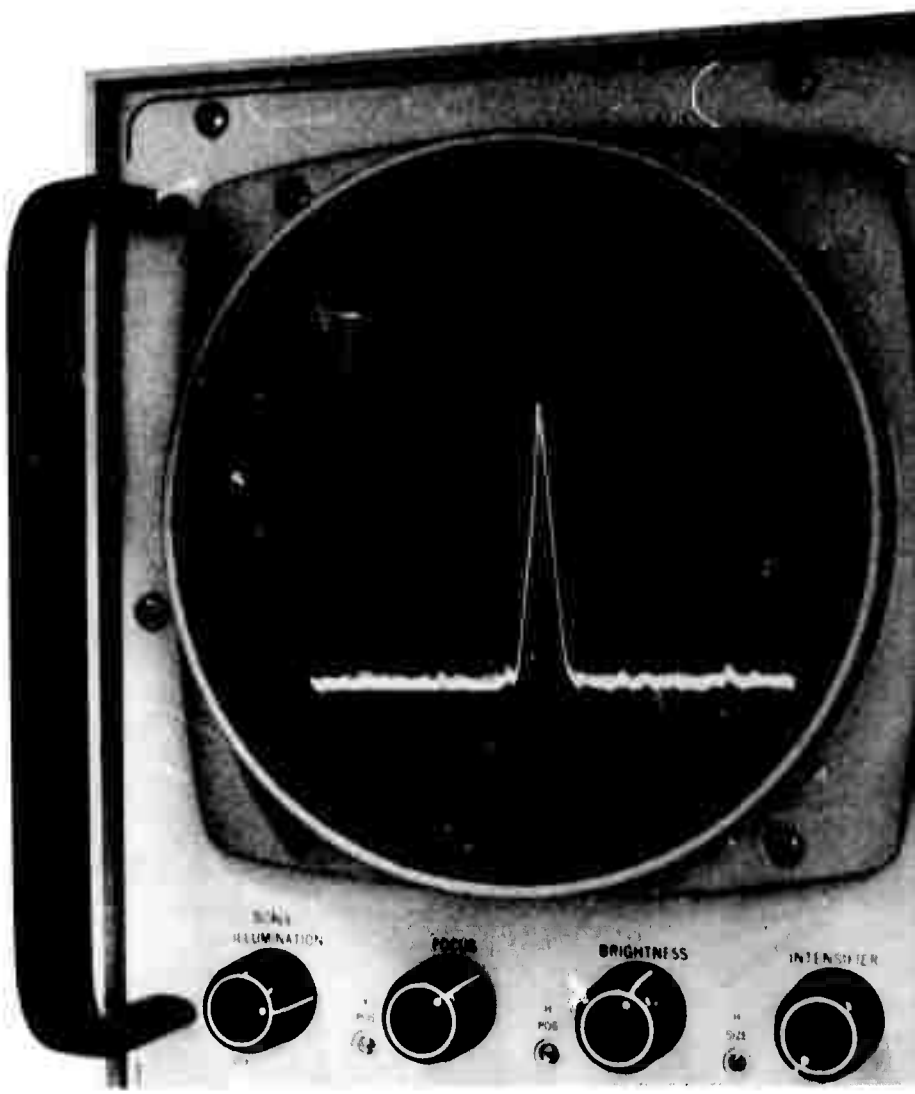

SCALE: Vertical 10dB/div; Horizontal 30 kHz/div.

NOT REPRODUCIBLE

HOLOBEAM,® INC.
LASER PRODUCTS DIVISION
560 WINTERS AVENUE ■ PARAMUS, NEW JERSEY 07652
TEL. 201-265-5335 ■ TWX. 710-990-4957

TM

Mode Locking a Nd:YAG Laser

Inserting a modulated loss element into a laser cavity generates highly stable subnanosecond pulses. Technique is also suited for second harmonic locking.

Improvements in the output of Nd:YAG lasers have induced incentives for harnessing this power. One such technique—mode locking—is particularly useful in building a source of coherent light for applications in high data-rate communications, nonlinear optics, and testing of high-speed photodetectors. This technique can also be used to produce a mode-locked second harmonic of a YAG laser (0.53 microns) to produce a train of green light pulses for such applications as underwater communications.

Mode locking creates a stable train of laser light pulses by modulating the internal loss of a laser at a frequency equal to the separation between adjacent longitudinal modes. The modes lock together with fixed relative amplitudes governed by the saturation of the active medium and with definite relative phases determined by the modulator. The laser converts its normal steady power output into a series of short pulses with a repetition frequency of $c/2\ell$ (the frequency separation of adjacent longitudinal modes for a laser cavity of length ℓ).

These pulses arise from the Fourier superposition of a large number of independent oscillating modes which have been forced to run with an exact harmonic and phase relationship, Figs. 1a and 1b.

How mode locking occurs

A more physical way of viewing the creation of the pulsed train is by recalling that a continuously pumped laser will always operate in equilibrium, with losses in the optical cavity at a minimum. Therefore by introducing a modulated loss element into the cavity, Fig. 2, the photons will "bunch up" and "sneak" through the modulator at maximum transmission. These pulses will persist as long as the modulator driving frequency is such that each pulse can make a "round trip" through the laser cavity or, $c/2\ell$.

The pulses will continue to decrease in width until the spectral width broadens to such an extent that the amplifying bandpass of the laser medium is no longer adequate. The laser then settles into a condition where the loss due to a passage of finite width pulses through the loss modulator is just equal to the loss sustained in passing spectrally broadened signals through a bandpass amplifier.

Loss modulation is obtained using Pockels cell or an acoustic diffraction cell within the cavity. In addition, loss can be introduced by modulating the phase of the optical signal within the laser cavity. Phase modulation causes an effective increase in the spectral width and therefore introduces a modulated loss through interaction with the amplifier bandpass.

Mode locking effectiveness

Mode locking of a pulse, propagated through a laser cavity, can be examined by considering the relationship between the modulation and the atomic line width, Fig. 3.

A Gaussian pulse with intial complex amplitude

$$f_1(t) = \exp\left[-\alpha t^2 + j\left(\omega_0 t + \beta t^2\right)\right] \quad (1)$$

is passed through a laser medium whose transfer function is (written to maintain Gaussian form):

$$g(\omega) = \exp\left\{\alpha_0 L\left[1 - j T_2(\omega - \omega_0) - T_2^2(\omega - \omega_0)^2\right]\right\} \quad (2)$$

The output pulse $f_2(t)$ is delayed and broadened but still Gaussian.

Passing this through the modulator, either a

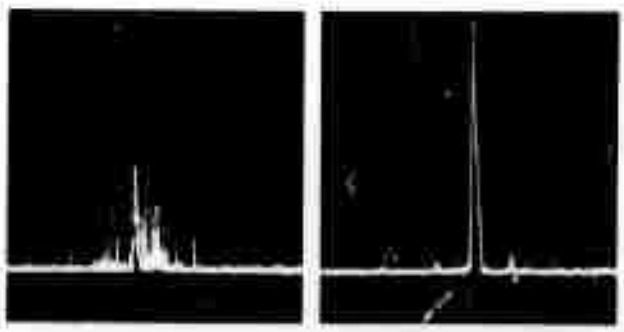

1. Cw laser output is displayed on the log scale of a spectrum analyzer; **(a)** represents normal output, **(b)** the mode locked output. Noise level is about 50 dB down.

Dr. James H. Boyden, Director, Laser Products Div., Holobeam, Inc., Paramus, N. J.

REPRINTED WITH PERMISSION FROM: **MICROWAVES • March, 1971**

phase modulator with a single pass phase delay of

$$\Delta\phi(t) = \delta \sin (2\pi\Delta f_{axial}\, t) \ , \qquad (3)$$

or a loss modulator with single pass transmission results in

$$T(t) = \exp [-2\,\delta\ell \sin^2(\pi\Delta f_{axial} t)] \ . \qquad (4)$$

Assuming the pulse passes through at the extreme of the modulation, the pulse after the modulator is

$$f_3(t) = f_2(t) \exp [-j2\delta(\pi\Delta f_{axial}\, t)^2)] \quad (5a)$$

$$f_3(t) = f_2(t) \exp [-2\,\delta\ell\,(\pi\Delta f_{axial} t)^2] \quad (5b)$$

Eq. 5a is for phase modulation (PM), while Eq. 5b applies to amplitude modulation (AM).

If the pulse shape is the same after one complete round trip, including frequency chirp, then

$$\alpha_{PM} \approx \beta_{PM} \approx \pi^2 (\delta/2g_o)^{1/2} \Delta f_{axial}\, \Delta f_{atomic} \quad (6a)$$

$$\tau_p(PM) = (2\,\ell n\, 2/\alpha)^{1/2} \approx [(2\,\ell n\, 2)^{1/2}/\pi]\ (2g_o/\delta)^{1/4} (1/\Delta f_{axial}\, \Delta f_{atomic})^{1/2} \qquad (6b)$$

where $g_o = 2\,\alpha\,L$ = saturated midband laser gain, τ_p = pulse width.

Similary,

$$\alpha_{AM} \approx \pi^2 (\delta\ell/2g_o)^{1/2}\, \Delta f_{axial}\, \Delta_{atomic} \qquad (7a)$$

$$\beta_{AM} = 0$$

$$\tau_p(AM) \simeq [(2\,\ell n\, 2)^{1/2}/\pi]\,(2g_o/\delta\ell)^{1/4} (1/\Delta f_{axial}\, \Delta f_{atomic})^{1/2} \qquad (7b)$$

These same relationships also apply to the laser operating at minimum loss.

From this analysis, several general scaling rules can be obtained:

- For a given modulation index δ or $\delta\ell$, the pulse and amplitude modulation cases will have the same pulse width τ_p. With pulse modulation, the locked spectrum of the laser, which is Gaussian, will have a bandwidth which will be larger by a factor of 1.4 because of the frequency chirp factor.
- For a given laser gain and modulation index the pulse width will be proportional to the square root of the cavity length.
- The pulse width is only weakly dependent upon the modulation index, $\delta\ell$ to the $-1/4$ power.

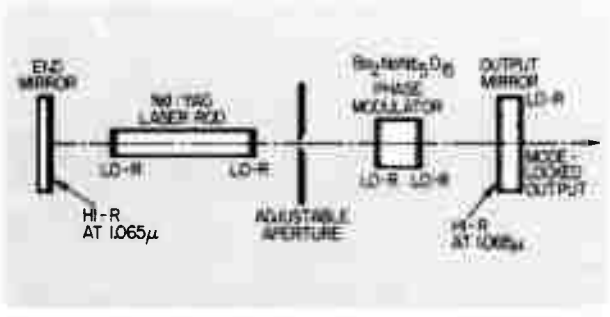

2. Mode locking of Nd:YAG laser is achieved by introducing a variable loss element which causes the photons to bunch-up into pulses and pass through the modulator at maximum transmission.

Crystals produce phase modulation

Phase modulation can be accomplished using an electro-optic modulator, usually lithium niobate or barium sodium niobate. The laser beam is propagated along the crystal's A or B axis and an electric field is impressed transverse to the beam. Typically a phase modulation index of approximately 0.1 results with 300 V across a 5 mm x 5 mm x 20 mm crystal. One of the advantages of phase modulation is that the crystal can be utilized along the same axis that is required for second harmonic generation.

Excellent mode-locking of a cw Nd:YAG laser can be obtained by using a tunable oscillator and adjusting the driving frequency to agree with the cavity length. Also, it is possible to alternately select a fixed frequency and adjust the mirror spacing to correspond.

Slow shifts in oscillator frequency and, more commonly, changes in effective cavity length due to thermal effects on the laser rod and laser support structure, will cause a gradual loss of resonance and a consequent increase in pulse width. It is therefore desirable to control the driving frequency of the mode-locking modulator using a reference derived from the laser itself. This can be accomplished by sensing the intermode beating with a high-speed photodetector and using this signal to control the mode-locking rf oscillator. The resultant mode-locking system is a closed-loop oscillator using the laser cavity as the basic reference, Fig. 4a. It automatically tracks changes in cavity geometry.

In a phase modulation system, Fig. 4b, there is a phase ambiguity between the laser pulse train and the modulator driving signal since

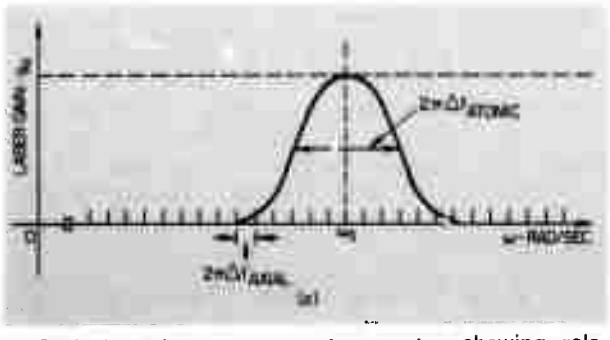

3. Optical cavity resonance frequencies showing relationship between modulation and the atomic line width; **(a)** $a_o = 2\,\pi\nu = 2\,\pi\,c/\lambda = 1.77 \times 10^{15}$ where c = velocity of light and λ = laser wavelength = 1.065 x 10^{-4} cm; **(b)** average optical power output = $f_1\, f_1^* = |f_1|^2$. $1/\Delta f_{axial} = 2\,\ell/c$ = round trip through cavity.

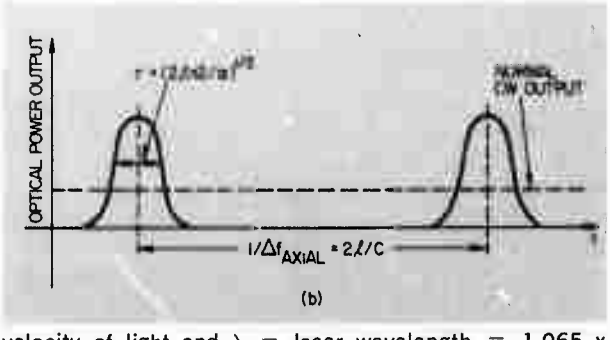

of residual reflections and optical interference effects in the laser cavity. Even small reflections from cavity elements can cause periodic enhancement of some of the longitudinal modes and increase the effective curvature of the gain profile at the atomic line center. This narrows the effective value of the atomic line width and broadens the related pulse widths.

Pulse width measurements of a mode-locked laser can be made in a variety of ways. The most accurate and unambiguous is with second harmonic generation techniques. When a continuous laser beam is passed through a non-linear crystal, such as barium sodium niobate or lithium iodate, and is converted into a mode-locked pulse train, the second harmonic power generated in the crystal increases by a ratio which is determined by the pulsewidth. If care is taken in accounting for the self-correlation which occurs between modes running with random phase in a normal cw laser, a rapid and precise measurement of pulsewidth can be obtained from the ratio of the second harmonic powers.

Another method for measuring pulsewidths is the use of a high speed photo diode such as an avalanche silicone detector and a sampling oscilloscope. However, the limiting resolutions with this approach is about 100 picoseconds, a factor of 2-3 larger than the values which can be produced ultimately with a cw Nd:YAG laser.

It is conceptually possible to determine pulsewidth by measuring the amplitudes and phases of the rf harmonics of the detected signal. In practice, however, this is very difficult. The amplitude of one or more of the high order harmonics, e.g., the 120th harmonic at 24 GHz of a 200 MHz mode-locked laser signal, varies as the mode-locking parameters are changed. Measurements show that changes of no more than 3 dB occur at these high order harmonics, indicating excellent pulse shape stability.

Other methods used for determining the effectiveness of mode locking include a rapid-scan Fabry-Perot spectrometer observation of the laser mode structure. A perfectly mode-locked homegeneous laser can have a Gaussian distribution of mode amplitude. Since the number of modes oscillating can exceed 100, it is not always possible to resolve the modes when the free spectral range gives a complete envelope distribution. Spurious reflections are obvious as modulations of a smooth envelope.

Mode locking at second harmonics

One application of mode locking is to enhance and stabilize the second harmonic power extracted from a laser. In external cavities, second harmonic generation enhancements in green output of up to 30 to 1 have been observed with ratios of 10 or 15 to 1 being typical.

Mode locking is effective because the pulsations yield a lower loss operation of the laser than a purely cw mode. However, as a result of these pulsations, the enhancement in second harmonic output tends to suppress harmonic pulsations. Here, the laser will find a regime for operation which yields the lowest overall loss. The mode-locked pulses when generating a green power can have a larger width and correspondingly lower power than for the pure mode-locking case.

Mode-locking loss modulation

For conditions where the second harmonic generation is weak with no significant change in pulse shape, or circulating power, the three average loss components are

- Loss in transversing modulator:
  $\overline{L}_M = (\delta\ell/\alpha)^{1/2}\,\pi\,\Delta f_{\text{axial}}$
- Loss due to second harmonic generation
  $\overline{L}_{shg} = 2\,K\,\overline{P}\,(\alpha/\pi)^{1/2}\,(1/\Delta f_{\text{axial}})$
- Loss due to finite line width
  $\overline{L}_{AT} = (2^{1/2}/\pi)\,g_o^{1/2}\,\alpha^{1/2}\,(1/\Delta f_{\text{atomic}})$

where K = coupling coefficient due to nonlinear crystal

P = one way circulating average power.

Total loss (ignoring fixed components):

$$\overline{L}_T = \overline{L}_M + \overline{L}_{shg} + \overline{L}_{AT}$$

The laser will operate where the partial derivative of total loss with respect to α is

$$\partial\,\overline{L}_T/\partial\,\alpha = 0.$$

which yields

$$\alpha = \frac{\pi^2(\delta\ell/2\,g_o)^{1/2}\,\Delta f_{\text{axial}}\,\Delta f_{\text{atomic}}}{1 + [(2\,\pi^{1/2}K\overline{P}/g_o^{1/2}]\,(\Delta f_{\text{atomic}}/\Delta f_{\text{axial}})}$$

The ratio of mode locked to normal (cw) second harmonic power is

$$R = P_2^{ML}\,P_2^{N} =$$

$$= \frac{\pi^{1/2}(\delta\ell/2g_o)^{1/4}(\Delta f_{\text{atomic}}/\Delta f_{\text{axial}})^{1/2}}{1 + (\pi/2g_o)^{1/2}(\overline{P}^{N}{}_{2v}/\overline{P})\;(\Delta f_{\text{atomic}}/\Delta f_{\text{axial}})^{1/2}}$$

If good nonlinear coupling is obtained, yielding green outputs with good conversion efficiency, the results must be modified to reflect a decrease in fundamental circulating power. This can produce a decrease in the effective enhancement ratio from an external value of 15:1 to a level of only 2:1 or less. In the extreme case of a cw laser with very efficient conversion to the second harmonic, the mode locking can actually reduce this second-harmonic output. Measurement results prove this to be the case. To obtain more assistance from mode locking in increasing the green output requires mode locking with a high modulation index. However, the gain in performance is very slow compared with the practical difficulties of rf crystal overheating. Apparently, those laser-crystal combinations which are lossy and inefficient converter systems can be assisted greatly by mode locking. Mode locking can always increase the effectiveness of harmonic generation when the doubling crystal is external to the laser cavity.

pulses pass through the modualtor at extreme voltage points. This causes difficulties in sensing the first-order intermode beat frequency used to determine the driving frequency. A loss modulation system does not suffer from such ambiguity problems. It does tend, however, to excite natural relaxation oscillations in the cw laser. These oscillations cause fluctuations in amlpitude, accompanied by damped oscillations at frequencies in the 30 to 150 kHz range.

A practical mode-locking system

A mode-locking control system that has proven to be quite stable and effective, Fig. 5, consists of a krypton arc pumped Nd:YAG rod, 3 mm in diameter and 50 mm long. The cavity contains a polarizing element and an adjustable aperture to produce operation with the fundamental transverse mode. The phase modulator is a barium sodium niobate crystal (5 mm cube) driven at the base by a tuned frequency stub with a 50 ohm 5 W source at 200 MHz. The source consists of a 5-W wideband transistor amplifier driven by a voltage controlled oscillator whose spurious outputs are maintained at least 60 to 70 dB below the primary signal.

A one per cent transmitting mirror at the rear end of the laser samples a portion of the laser beam aimed at an avalanche photodiode with a characteristic gain-bandwidth product of 80 GHz. The resultant amplified 400 MHz signal is compared in a phase detector with a 400 MHz comparison signal derived by multiplying the output of the VCO by 2. The phase-detected output is amplified and is used to control the VCO.

Initial locking is performed manually by adjusting the bias on the VCO. Once the system is locked, it is maintained over a cavity length change of several megahertz, or about five per cent. Visual indication of lock is provided by a back-lit indicating pilot light and an easy-to-read phase level meter. A light indicates if AGC is adequate and system noise is minimal. Such a system produces pulse width on the order of 100 ps and will maintain lock for as long as the laser is left on.

To ensure the stability of the loop at the desired frequency, it is necessary to provide a variable phase adjustment. This adjustment, required during initial set-up, is obtained by sliding the photodetector on the optical rail or by changing the length of the cable betwen the photodetector and the modelocking electronics. Stable mode locking requires the phase shift vs frequency to be quite small over several megahertz. Therefore wideband amplifiers and filters are used.

Precautions must be taken to avoid residual acoustic effects within the crystal modulator which can accidentally introduce excessive relaxation oscillations.

Practical mode-locking tips

One of the most important considerations in a practical mode-locking system is the elimination

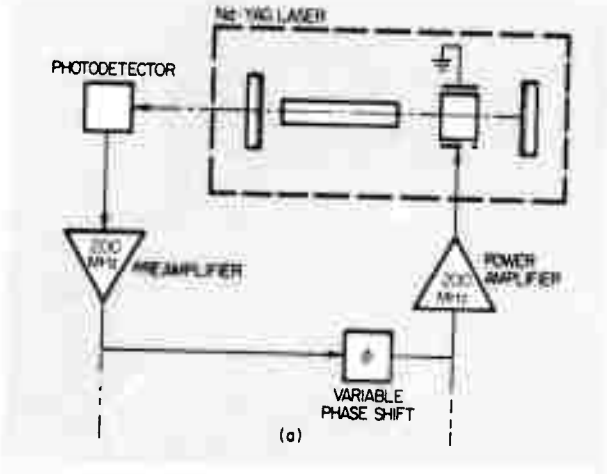

4. A simple mode locking system uses the laser itself as the oscillator, **(a)**. Ambiguity in the phase relationship between the laser pulse train and the modulator driving signal that can occur in (a) is avoided in **(b)** by using the second harmonic of the output signal, 400 MHz.

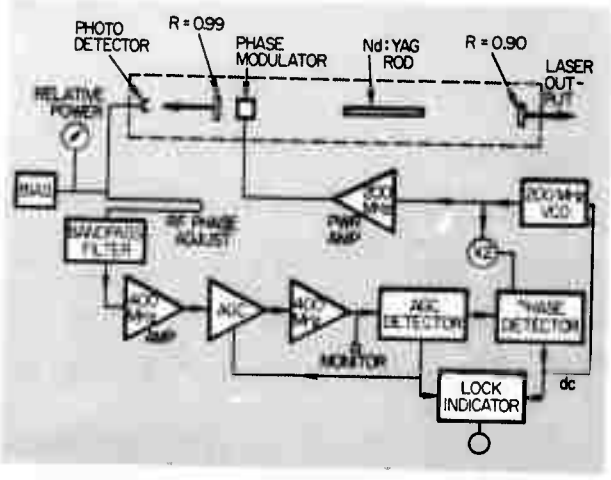

5. Mode locking system, Holobeam Model 250, uses solid state components throughout. The 400 MHz signal received by the photodiode is passed through a 10 MHz flat top filter, amplifier, AGC amplifier, another amplifier and then is phase detected.

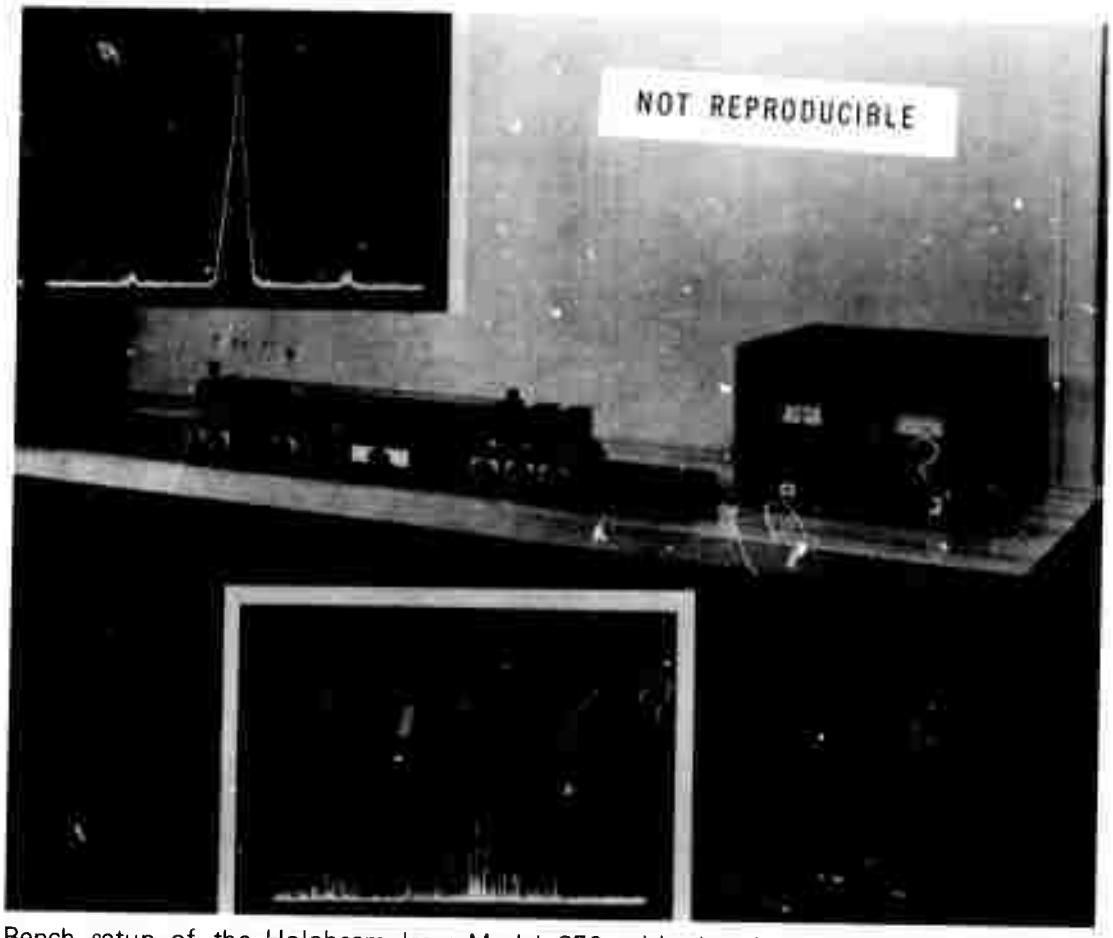

Bench setup of the Holobeam laser Model 250 with the electronic control cabinet for mode-locking. The bottom insert shows the laser running free, and the top insert the mode-locked output. Comparison shows that spurious signal levels are down 60 db.

Functional specifications, Holobeam mode-locking system

Operation	Fully automatic, closed loop
Power output	3-5 W, TEM_{00}
Frequency range (2% tuning range)	75-500 MHz (75, 100, 200 MHz standard, other frequencies optional)
Modulation type	Phase
Wavelength	1.064 microns (0.0532 optional)
Optical pulsewidth	Less than 150 picoseconds
Laser medium	Nd:YAG
Power input	208 Vac for the laser system, 120 Vac for the control electronics
Non-locked power	40 watts, multimode

HOLOBEAM®, INC.
LASER PRODUCTS DIVISION
560 WINTERS AVENUE ■ PARAMUS, NEW JERSEY 07652
TEL. 201-265-5335 ■ TWX. 710-990-4957

TM